FORSCHUNGSZENTRUM KARLSRUHE

Technik und Umwelt

Wissenschaftliche Berichte

FZKA 6619

STELLAR NEUTRON CAPTURE CROSS SECTIONS OF THE Cd ISOTOPES

K. WISSHAK, F. VOSS, F. KÄPPELER, and L. KAZAKOV[1]

Institut für Kernphysik

[1]Institute for Physics and Power Engineering, Obninsk–Kaluga Region, Russia

Forschungszentrum Karlsruhe GmbH, Karlsruhe
2001

ABSTRACT

The neutron capture cross sections of ^{110}Cd, ^{111}Cd, ^{112}Cd, ^{113}Cd, ^{114}Cd, and ^{116}Cd have been measured in the energy range from 3 to 225 keV at the Karlsruhe 3.75 MV Van de Graaff accelerator. Neutrons were produced via the ^{7}Li$(p,n)^{7}$Be reaction by bombarding metallic Li targets with a pulsed proton beam. The Karlsruhe 4π Barium Fluoride Detector was used for registration of capture events. The cross sections were determined relative to the gold standard using highly enriched metallic Cd samples. The respective ratios could be obtained with overall uncertainties between 0.8 and 1.6%, about an order of magnitude more accurate than previous data. Maxwellian averaged neutron capture cross sections were calculated for thermal energies between $kT = 8$ keV and 100 keV. For three isotopes the results agree fairly well with a recent evaluation, while the other cases differ by 30 - 40%.

ZUSAMMENFASSUNG

DIE STELLAREN (n,γ) QUERSCHNITTE DER Cd ISOTOPE

Die Neutroneneinfangquerschnitte von ^{110}Cd, ^{111}Cd, ^{112}Cd, ^{113}Cd, ^{114}Cd und ^{116}Cd wurden am Karlsruher Van de Graaff Beschleuniger im Energiebereich von 3 bis 225 keV gemessen. Neutronen wurden über die ^{7}Li$(p,n)^{7}$Be–Reaktion durch Beschuss metallischer Li–Targets mit einem gepulsten Protonenstrahl erzeugt, und Einfangereignisse mit dem Karlsruher 4π Barium Fluorid Detektor nachgewiesen. Die Messung wurde relativ zum (n,γ)–Querschnitt von Gold als Standard mittels hochangereicherter, metallischer Cd-Proben durchgeführt. Die Unsicherheiten der resultierenden Querschnittsverhältnisse liegen zwischen 0.8 und 1.6%, und sind damit um eine Größenordnung genauer als frühere Ergebnisse. Die stellaren Einfangquerschnitte wurden für thermische Energien von $kT = 8$ keV bis 100 keV berechnet. Für drei der untersuchten Isotope stimmen die Ergebnisse gut mit einer neueren Evaluation überein, wogegen die anderen Werte um 30 - 40% differieren.

Contents

1 INTRODUCTION

The present measurement of the (n,γ) cross sections of the cadmium isotopes is part of a comprehensive study with the Karlsruhe $4\pi BaF_2$ detector for investigating the isotopes of the main s-process component. The present data - and the results of a recent experiment on the relevant xenon isotopes - are providing an almost complete set of accurate cross sections in the mass range from ^{110}Cd to ^{170}Yb, including all s-only isotopes except ^{164}Er. In total, 52 isotopes have been investigated, the respective results being included in a recent update of evaluated stellar (n,γ) rates [1].

The s-process reaction path in the vicinity of cadmium is sketched in Fig. 1. The s-only isotope ^{110}Cd, which is shielded against the β-decay chains from the r-process region by its stable Pd isobar, is an important normalization point for the overall abundance distribution because it is not affected by possible branchings. Hence its abundance represents the full s-process flow, similar to ^{124}Te and ^{150}Sm.

The previous experimental information on the cadmium isotopes is relatively poor. The only complete set of cross sections by Musgrove *et al.* was reported in two slightly different versions [2, 3], and was later renormalized using correction factors published in Ref. [4]. These data are quoted with uncertainties of 12 - 15% and are, therefore, not adequate for a detailed s-process analysis. The result for ^{110}Cd obtained in an earlier study by Stroud [5] was consistent with the data of Musgrove *et al.* but showed similar uncertainties. In a recent activation experiment Theis *et al.* [6] investigated a series of isotopes, i.e. ^{114}Cd, ^{116}Cd, and the rare isotopes outside the s-path, ^{106}Cd and ^{108}Cd. These results are quoted with comparably small uncertainties of 3-4%.

Cross section measurements on the even cadmium isotopes are complicated by the fact that neutron capture may significantly populate a number of isomers. For conventional techniques based on Moxon-Rae type detectors or on total energy detectors with pulse height weighting, this feature implies inherent uncertainties, which can not be quantified. These techniques do not allow to distinguish capture cascades feeding the ground state or the isomer, but are using the sum energy of the capture cascade - represented by the binding energy of the captured neutron plus its comparably small kinetic energy - as a fixed parameter. Accordingly, events leading to the isomer are evaluated with binding energies, that are too high. This effect may well cause systematic uncertainties of the order of 10% as was recently observed for the ytterbium isotopes [7].

Capture to an isomeric state could affect the important cross section of ^{110}Cd if the isomeric state in ^{111}Cd at 396 keV excitation energy is sufficiently fed. The present experimental technique is insensitive to this problem, since the efficiency for capture cascades to the ground state and to the isomer is almost identical. Moreover, the good resolution in γ-energy allows direct detection of any significant feeding for isomeric states above 250 keV excitation energy as is the case for ^{110}Cd and ^{112}Cd.

Measurements and data analysis are described in Secs. 2 and 3, followed by a discussion

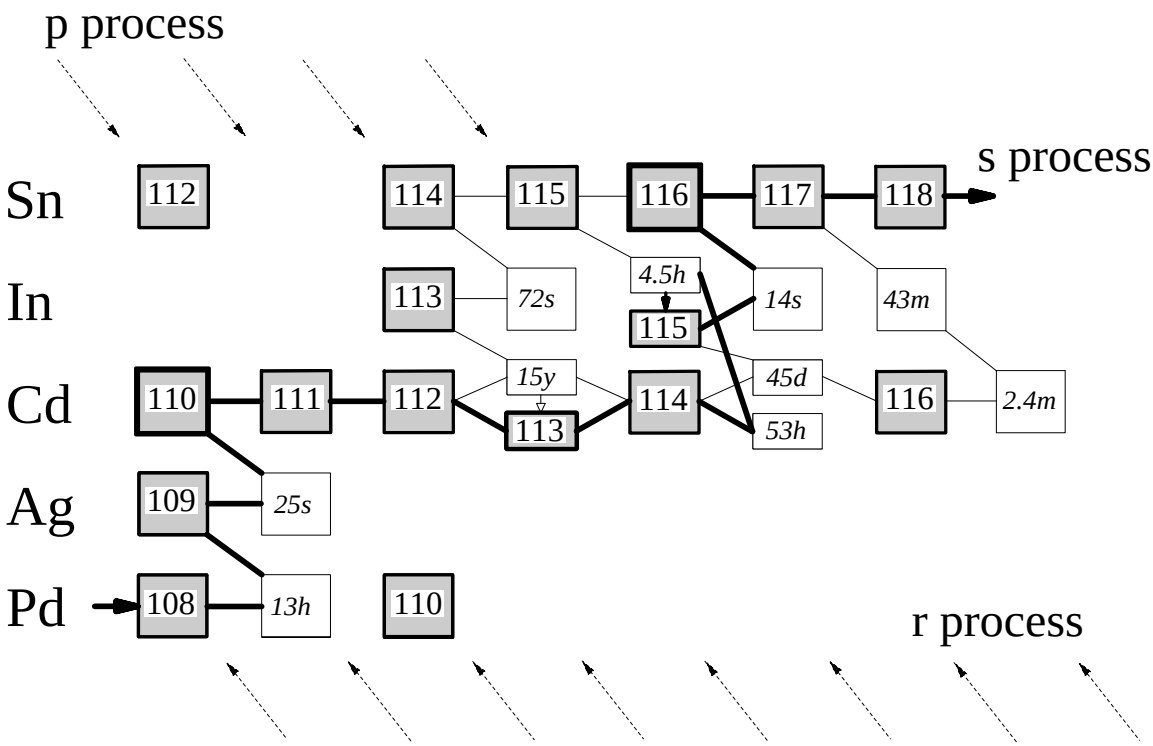

Figure 1: The reaction path of the s process in the region of the cadmium isotopes. Relevant isomeric states are indicated by separate boxes. Note that ^{110}Cd and ^{16}Sn represent s-only isotopes since they are shielded against β-decays from the r -process region.

of the results and uncertainties in Secs. 4 and 5. The stellar cross sections are presented in Sec. 6. The astrophysical implications will be addressed in a forthcoming publication.

2 EXPERIMENT

The neutron capture cross sections of the cadmium isotopes 110 to 114 and 116 have been measured in the energy range from 3 to 225 keV using gold as a standard. Since the experimental method has been published in detail [8, 9, 10, 11], only a general description is given here, complemented with the specific features of the present measurement.

Neutrons were produced via the ^{7}Li$(p,n)^7$Be reaction by bombarding metallic Li targets with the pulsed proton beam of the Karlsruhe 3.75 MV Van de Graaff accelerator. The neutron energy was determined by time of flight (TOF), the samples being located at a flight path of 79 cm. The relevant parameters of the accelerator were a pulse width of <1 ns, a repetition rate of 250 kHz, and an average beam current of 2.2 μA. In different runs, the proton energies were adjusted 30 and 100 keV above the threshold of the ^{7}Li$(p,n)^7$Be reaction at 1.881 MeV. In this way, continuous neutron spectra in the proper energy range for s–process studies were obtained, ranging from 3 to 100 keV, and 3 to 225 keV, respectively. The lower maximum neutron energy offers a significantly better

signal-to-background ratio at lower energies.

Capture events were registered with the Karlsruhe 4π Barium Fluoride Detector via the prompt capture γ–ray cascades. This detector consists of 42 hexagonal and pentagonal crystals forming a spherical shell of BaF_2 with 10 cm inner radius and 15 cm thickness. It is characterized by a resolution in γ–ray energy of 7% at 2.5 MeV, a time resolution of 500 ps, and a peak efficiency of 90% at 1 MeV. The 1.6 MeV threshold in γ–ray energy used in the present experiment corresponds to an efficiency for capture events of more than 95% for all investigated isotopes. A comprehensive description of this detector can be found in Ref. [10].

The experiment was divided into three runs, two using the conventional data acquisition technique with the detector operated as a calorimeter, and one with an analog-to-digital converter (ADC) system coupled to the detector for analyzing the signals from all modules individually. In this way, the full spectroscopic information recorded by the detector can be recovered.

The cadmium samples were prepared from isotopically enriched metal pieces which were pressed into pellets of 15 mm diameter, which could be used without any additional canning. Apart from the 6 cadmium samples, a gold sample was used for measuring the neutron flux and an empty position in the sample ladder for determining the sample independent background. A carbon sample served for simulating the background due to scattered neutrons. The relevant sample parameters are compiled in Table 1, and the isotopic composition of the cadmium samples provided by IPPE Obninsk is listed in Table 2.

The neutron transmission of the samples calculated with the SESH code [12] was generally larger than 90% (Table 3). The measured spectra of all samples were normalized to equal neutron flux by means of a ^{6}Li–glass monitor located close to the neutron target. The transmission spectra measured with a second ^{6}Li–glass detector at a flight path of 260 cm were used for a rough determination of the total cross sections. Though the accuracy of this method is inferior to that obtained in a dedicated experiment, these total cross sections can be used in the calculation of the multiple scattering correction.

The samples were moved cyclically into the measuring position by a computer controlled sample changer. The data acquisition time per sample was about 10 min, a complete cycle lasting about 1.3 h. From each event, a 64 bit word was recorded on DAT tape containing the sum energy and TOF information together with 42 bits identifying the contributing detector modules. The respective parameters of the three runs corresponding to neutron spectra with different maximum energies are listed in Table 4. The data in run I were recorded with the ADC system.

Table 1: SAMPLE CHARACTERISTICS

Sample	Diameter	Thickness		Weight	Neutron binding
	(mm)	(mm)	$(10^{-3}$at/barn$)^a$	(g)	energy (MeV)
^{114}Cd	14.8	2.7	11.941	3.9942	6.141
Graphite	15.0	1.5	13.364	0.4710	
^{113}Cd	14.8	0.7	2.9615	0.9820	9.043
^{110}Cd	14.8	1.7	7.7312	2.4978	6.976
^{197}Au	15.0	0.4	2.2470	1.2987	6.512
^{112}Cd	14.8	1.7	7.5789	2.4913	6.540
^{111}Cd	14.8	1.5	6.4349	2.0971	9.398
Empty					
^{116}Cd	14.8	4.0	17.603	5.9796	5.777

[a]For cadmium samples: sum of all Cd isotopes

Table 2: ISOTOPIC COMPOSITION (%)

Sample	Isotope					
	^{110}Cd	^{111}Cd	^{112}Cd	^{113}Cd	^{114}Cd	^{116}Cd
^{110}Cd	95.51	1.59	1.35	0.50	0.91	0.14
^{111}Cd	0.34	95.92	2.16	0.49	0.96	0.13
^{112}Cd	0.09	0.21	97.92	0.91	0.78	0.09
^{113}Cd	0.12	0.18	1.71	95.33	2.45	0.21
^{114}Cd	0.07	0.09	0.28	0.26	99.07	0.23
^{116}Cd	0.57	0.60	1.72	1.10	3.61	92.40

3 DATA ANALYSIS

3.1 Total Cross Sections

The total cross sections of the investigated isotopes were determined in the neutron energy range from 10 to 200 keV via the TOF spectra measured with the ^{6}Li glass detector at a flight path of 260 cm. The total cross sections and the related uncertainties were obtained as described in Ref. [8], and are listed in Table 5. The results deduced for the carbon sample agree with the data from the Joint Evaluated File (JEF) [13] within $\pm$4.0%. The quoted uncertainties were obtained under the assumption that they are inversly proportional to the fraction of neutrons interacting in the sample, $A = 1 - T$, where T is the transmission. For the carbon sample this fraction is A=5.8%, the related uncertainty of 4.0% being estimated from the comparison with the JEF data. The cross section for elemental cadmium, which was calculated from the isotopic contributions with the assumption that the rare isotopes ^{106}Cd and ^{108}Cd have the same cross section as ^{110}Cd, was found in reasonable agreement with the data given in Ref. [14], the present

Table 3: CALCULATED NEUTRON TRANSMISSION[a]

Sample	Neutron Energy (keV)				
	10	20	40	80	160
^{197}Au	0.959	0.965	0.970	0.974	0.979
^{110}Cd	0.949	0.949	0.949	0.949	0.948
^{111}Cd	0.954	0.955	0.956	0.956	0.955
^{112}Cd	0.952	0.952	0.951	0.949	0.947
^{113}Cd	0.976	0.977	0.977	0.976	0.975
^{114}Cd	0.927	0.926	0.923	0.920	0.917
^{116}Cd	0.914	0.911	0.906	0.900	0.894

[a] Monte Carlo calculation with SESH code [12].

Table 4: PARAMETERS OF THE INDIVIDUAL RUNS

Run	Flight Path (mm)	TOF Scale (ns/ch)	Number of Cycles	Maximum Neutron Energy (keV)	Measuring Time (d)	Mode of Operation	Average Beam Current (μA)	Threshold in Sum Energy (MeV)
I	787.8	0.7092	340	100	16.2	ADC	2.4	1.6
II	788.0	0.7601	283	100	17.1	Calorimeter	2.1	1.8
III	787.9	0.7602	280	200	13.9	Calorimeter	2.2	1.7

data beeing systematically larger by $\sim 5\%$ compared to the ENDF/B-V evaluation. This difference, however, is well compatible with the quoted uncertainties.

3.2 Capture Cross Sections

The analysis was carried out in the same way as described previously [8, 9, 11]. All events were sorted into two–dimensional spectra containing 128 sum energy versus 2048 TOF channels according to different multiplicities (evaluation 1). In evaluation 2, this procedure was repeated by rejecting those events, where only neighboring detector modules contributed to the sum energy signal. With this option, background from the natural radioactivity of the BaF_2 crystals and from scattered neutrons can be reduced. For all samples, the resulting spectra were normalized to equal neutron flux using the count rate of the ^{6}Li glass monitor close to the neutron target. The corresponding normalization factors are below 0.5% for all runs. The treatment of the two-dimensional spectra from the data recorded with the ADC system is slightly more complicated and was performed as described in Ref. [8].

In the next step of data analysis, sample-independent backgrounds were removed by subtracting spectra measured with the empty position in the sample changer frame. A remaining constant background was determined at very long flight times, where no time-

Table 5: MEASURED TOTAL CROSS SECTIONS [a]

Neutron Energy	Total Cross Section (barn)							
(keV)	^{110}Cd	^{111}Cd	^{112}Cd	^{113}Cd	^{114}Cd	^{116}Cd	^{12}C	^{197}Au
10 – 15	6.0	7.4	6.5	8.0	6.3	4.8	4.47	12.9
15 – 20	7.8	7.4	6.9	9.6	7.1	6.2	4.98	15.4
20 – 30	7.1	6.8	6.8	8.5	6.6	6.1	4.78	13.6
30 – 40	6.8	7.3	6.5	8.7	7.2	5.6	4.74	12.5
40 – 60	7.2	7.3	6.8	8.9	7.2	6.7	4.75	11.6
60 – 80	7.6	7.3	7.2	9.1	7.5	6.6	4.68	11.3
80 – 100	7.8	7.3	7.2	8.0	7.2	7.1	4.58	10.6
100 – 150	7.2	7.8	7.4	8.6	7.5	7.2	4.40	10.5
150 – 200	7.6	7.6	7.5	7.9	7.4	7.1	4.15	9.8
Typical Uncertainty (%)	4.1	4.7	4.5	9.3	2.9	2.1	4.0	8.0

[a]Determined from the count rate of the ^{6}Li glass neutron monitor at 260 cm flight path

correlated events are expected. The resulting two-dimensional spectra for events with multiplicity >2 measured in run I are shown for all investigated isotopes in Figs. 2, 3, and 4. Note that events with low sum energy and large TOF are suppressed by a preprocessing option of the ADC system.

At this point, the spectra contain only events correlated with the sample. The next correction to be made is for isotopic impurities (see Ref.[8] for details). The respective coefficients are compiled in Table 6. Fig. 5 shows the TOF spectrum of the ^{116}Cd sample before subtraction of the background from isotopic impurities together with this background. In this case the correction is about 13% of the measured effect, but for all other samples it is below 5%.

Following the correction for isotopic impurities, the background due to capture of sample scattered neutrons was removed from the spectra by means of the data measured with the scattering sample. The binding energy of the even isotopes is low enough, that the correction can be normalized using the pronounced peak in the sum-energy spectra at 9.1 MeV due to capture in the odd barium isotopes ^{133}Ba and ^{135}Ba (see Figs. 2 to 4).

In case of the odd isotopes, however, this peak can not be distinguished from the full energy peak of the respective Cd isotope. Therefore, the normalization had to be based on the peak due to capture in the even barium isotopes at 6.8 MeV, which, however, overlaps with the tail of the true capture spectrum, thus resulting in a somewhat larger uncertainty of this correction (for details see Ref. [9]).

After this last correction, the final spectra contain only the net capture events of the investigated isotopes (bottom spectra in Figs. 2, 3, and 4). The corrections for capture of scattered neutrons are shown for all measured isotopes in Fig. 6, and the corresponding signal/background ratios are listed for different neutron energies in Table 7.

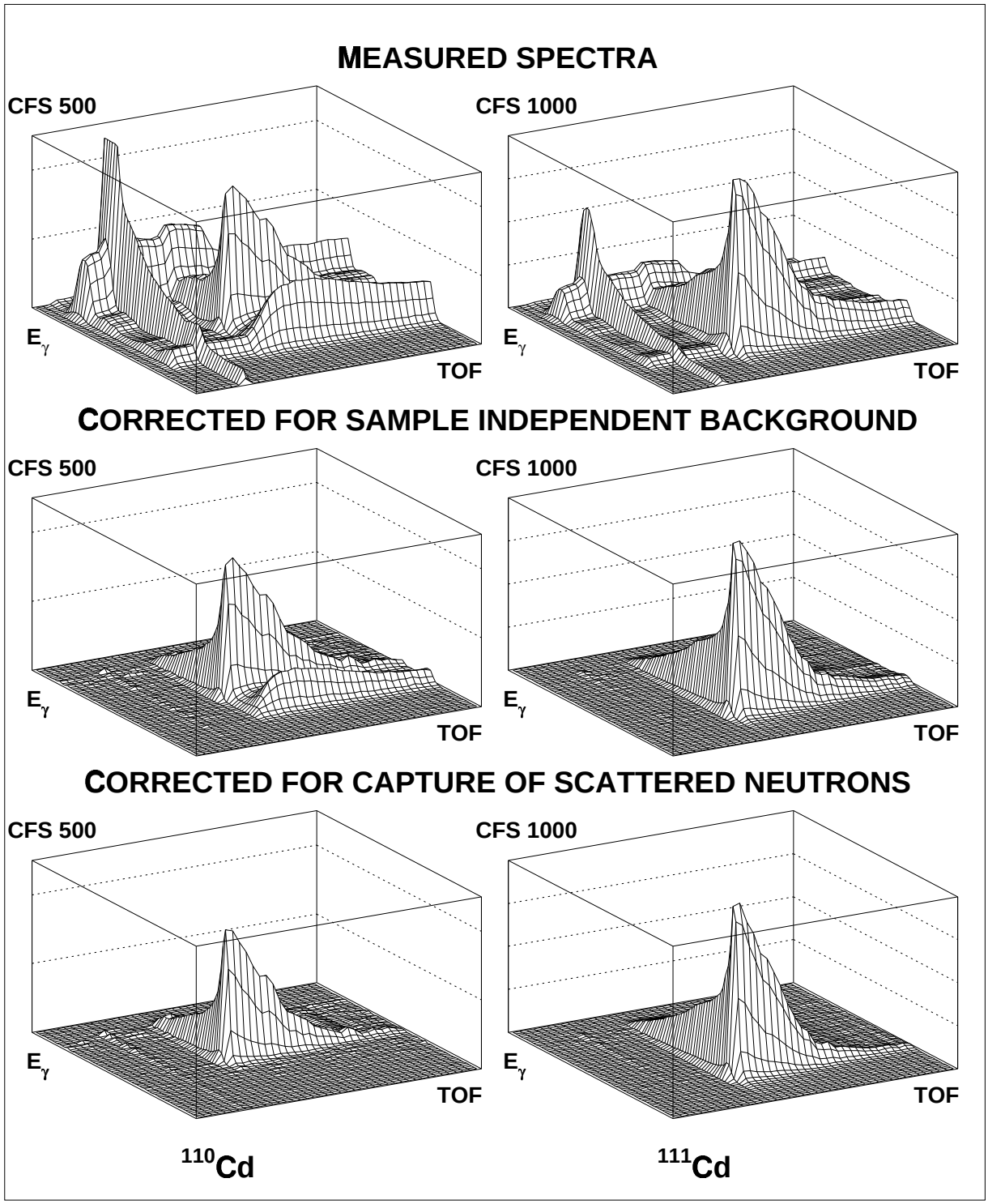

Figure 2: The different steps of background subtraction in the two–dimensional sum energy × TOF spectra. The data are shown for ^{110}Cd and ^{111}Cd measured with the ADC system in run I with 100 keV maximum neutron energy. Only the events with multiplicity >2 are shown. (The original resolution of 128 × 2048 channels was compressed into 64 × 64 channels for better readability. Events at low sum-energy and large TOF are suppressed by the preprocessing in the ADC system.)

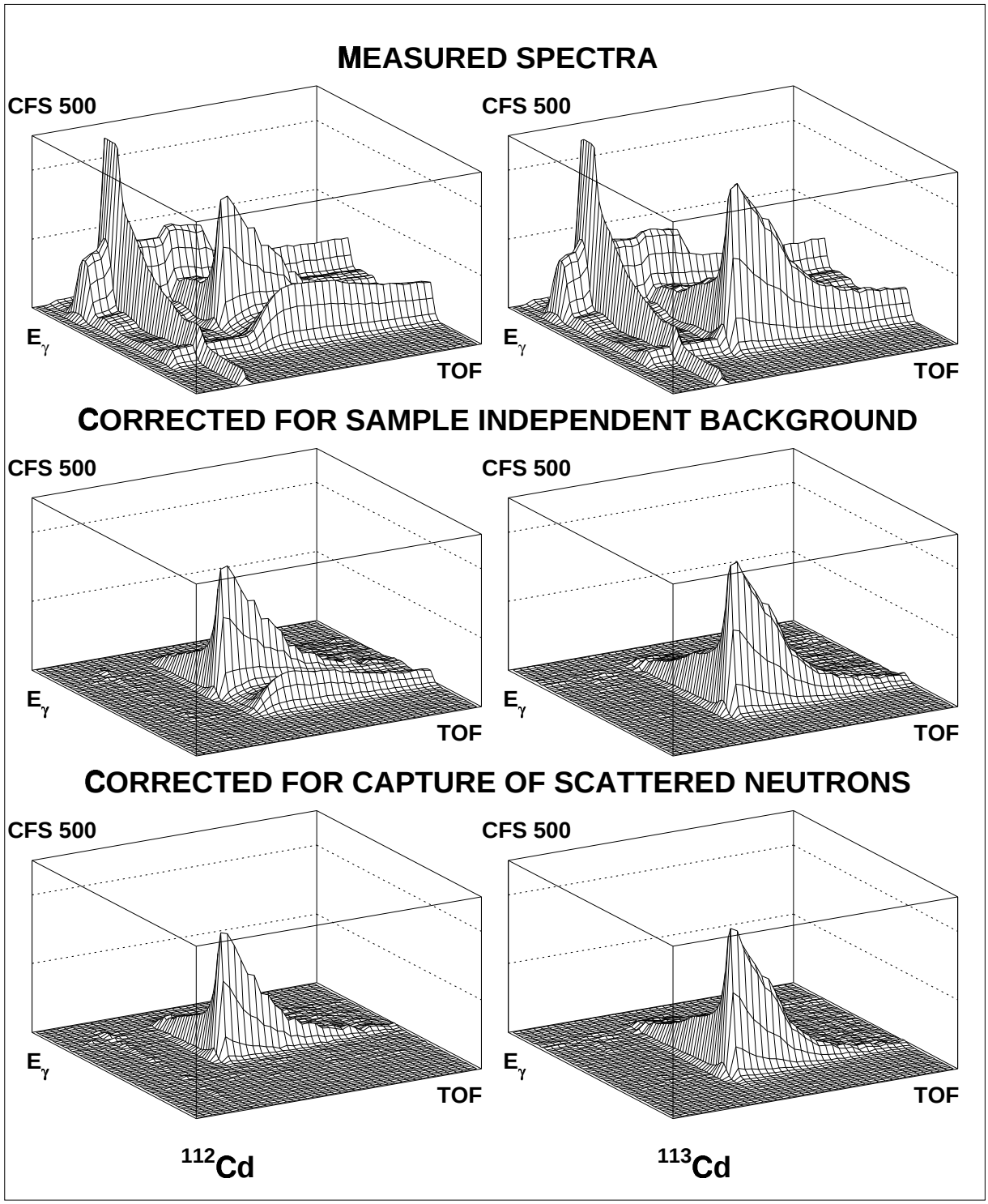

Figure 3: As Fig. 2 but for the ^{112}Cd and ^{113}Cd samples.

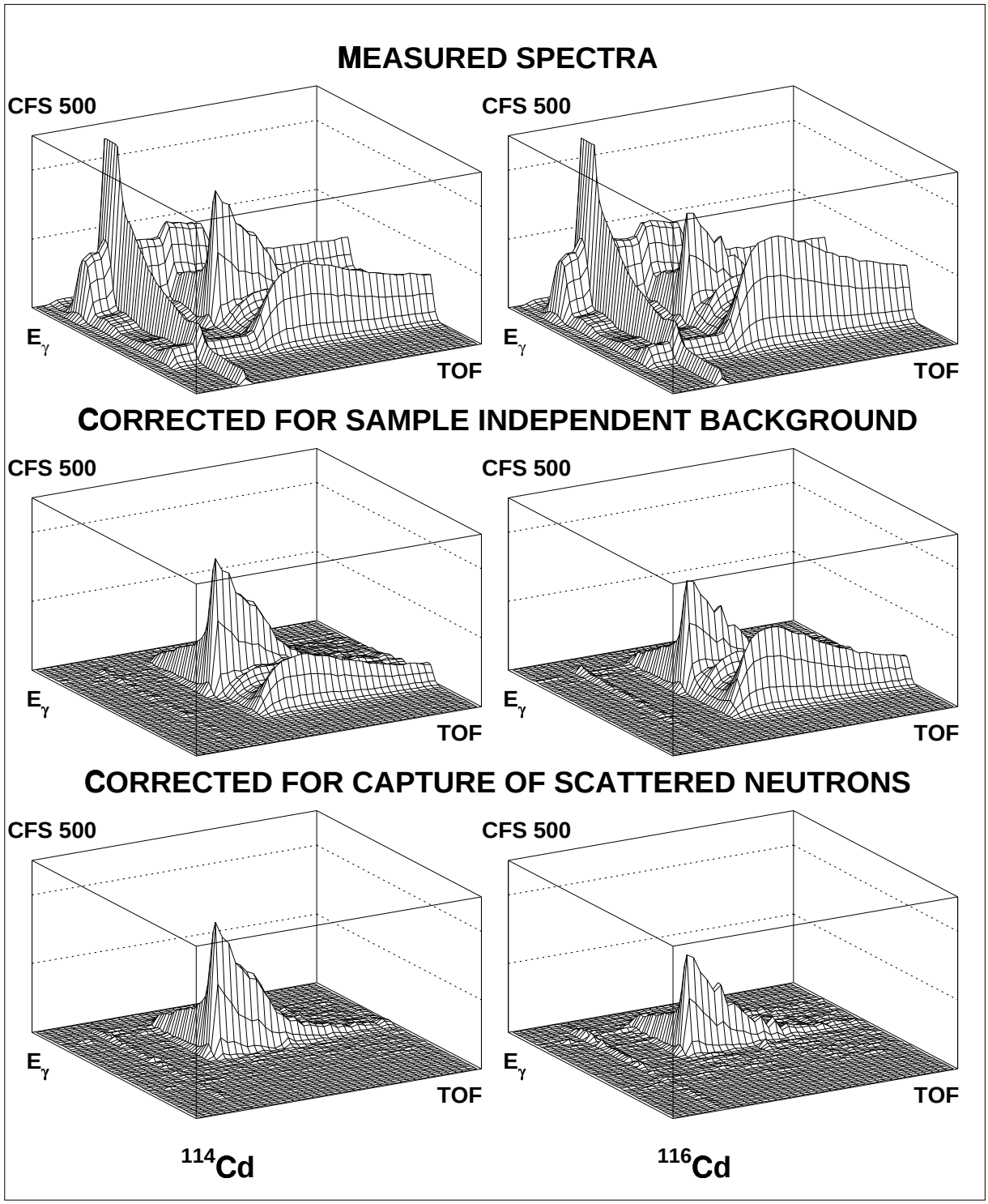

Figure 4: As Fig. 2 but for the ^{114}Cd and ^{116}Cd samples.

The resulting sum-energy spectra of Fig. 7 demonstrate an important feature of the present setup: Comparison of the spectra in Fig. 6 show that similar signal to background ratios could be obtained for all isotopes in spite of the fact, that the capture/scattering ratios at 30 keV vary by an order of magnitude, between 9 for ^{111}Cd and 94 for ^{116}Cd (see Table 7). The better background suppression in case of ^{116}Cd is possible because its binding energy of 5.7 MeV is lower than for all barium isotopes. Hence, the sum energy peak is located below the corresponding Ba peaks and is, therefore, much less disturbed by this background, in contrast to the situation for the odd Cd isotopes, where this discrimination is hampered by the high binding energies.

After subtraction of the scattering background the cross section shape versus neutron energy was determined from the TOF spectra of Fig. 6. These spectra are calculated by integrating the two-dimensional spectra in a region around the full energy peak. The different background conditions in the spectra of events with different multiplicities, this range was chosen to decrease with multiplicity (see Fig. 8). For normalization, the two–dimensional data were projected onto the sum energy axis using the TOF region with optimum signal/background ratio as indicated in Fig. 6 by two vertical lines. The resulting pulse height spectra are shown in Fig. 7 for the events with multiplicity >2. The threshold in sum energy is 1.7 MeV.

Table 6: MATRIX FOR ISOTOPIC CORRECTIONS (%)

Corrected spectrum	Measured spectrum						Corrected sample thickness
	^{110}Cd	^{111}Cd	^{112}Cd	^{113}Cd	^{114}Cd	^{116}Cd	(10^{-3} at/barn)
^{110}Cd	100	–1.985	–1.355	–1.304	–0.566	–0.064	7.3834
^{111}Cd	–0.293	100	–1.857	–1.059	–0.502	–0.049	6.1715
^{112}Cd	–0.089	–0.253	100	–2.431	–0.481	–0.040	7.4193
^{113}Cd	–0.046	–0.082	–0.676	100	–0.607	–0.037	2.8224
^{114}Cd	–0.110	–0.167	–0.432	–1.074	100	–0.168	11.827
^{116}Cd	–1.341	–1.659	–3.961	–6.667	–5.294	100	16.263

Capture events are defined by summing the signals from the various BaF_2 modules within a time interval of ∼10 ns. Thus, capture cascades leading to a longer-lived isomeric state do not contain the full binding energy of the captured neutron, the respective events being registered with correspondingly lower sum energies. If capture on the even cadmium isotopes would populate the isomeric states with spin $11/2^-$, the good energy resolution of the detector should allow to identify the respective partial cross sections, similar to the findings for the ytterbium isotopes [7]. Though the resolution was sufficient for the higher-lying isomers in ^{111}Cd and ^{117}Cd at 396 and 264 keV, Fig. 7 shows no indication for a significant population, presumably due to the high spin of these isomers. Only the full energy peak of ^{110}Cd appears to be slightly broadened, well compatible with the 6% population of the isomer found in an activation experiment [6].

The sum energy spectra of all isotopes are shown in Fig. 8 for different multiplicities. These multiplicities correspond to the number of detector modules contributing per event, which are slightly larger than the true multiplicities because of cross talking. In the even

Table 7: SIGNAL/BACKGROUND RATIO FOR RUNS WITH DIFFERENT MAXIMUM NEUTRON ENERGY

Sample	σ_t/σ_γ	Maximum neutron energy	Signal/Background ratio[a]		
	E_n=30 keV	(keV)	E_n=30 keV	E_n=20 keV	E_n=10 keV
^{110}Cd	31	100	5.0	2.8	2.0
^{111}Cd	9		8.4	4.4	2.2
^{112}Cd	41		5.0	2.9	2.0
^{113}Cd	12		7.8	4.1	2.1
^{114}Cd	58		5.5	2.9	2.0
^{116}Cd	94		3.8	2.5	1.6
^{197}Au	24		8.8	4.4	2.8
^{110}Cd		200	3.8	2.5	1.7
^{111}Cd			5.6	3.3	2.1
^{112}Cd			3.6	2.4	1.6
^{113}Cd			4.8	2.9	1.9
^{114}Cd			4.2	2.5	1.8
^{116}Cd			2.9	2.0	1.4
^{197}Au			7.0	3.5	2.3

[a]Defined as (effect+neutron scattering background)/(neutron scattering background)

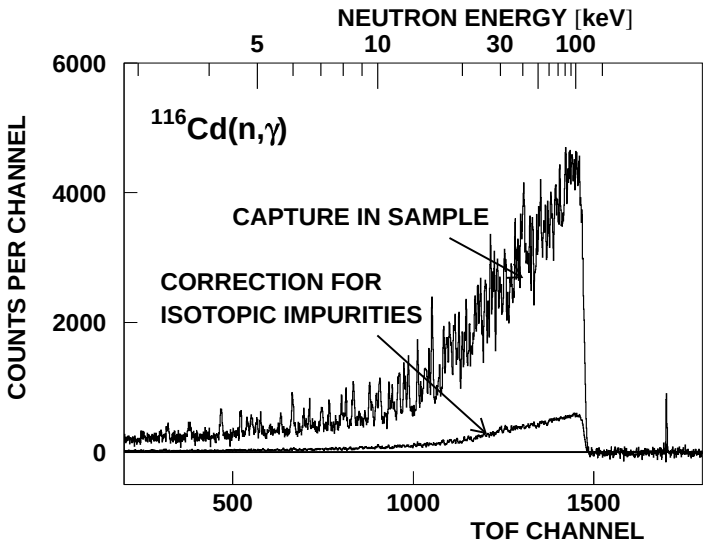

Figure 5: TOF spectrum of the ^{116}Cd sample. The background due to isotopic impurities is shown separately.

cadmium isotopes, 30 to 45% of the capture events are observed with multiplicities ≥ 5, while the respective fraction in the odd isotopes is about 65%. The arrows in Fig. 8 indicate the range of sum energy channels that were integrated to obtain the TOF spectra of Fig. 6 for determining the cross section shapes.

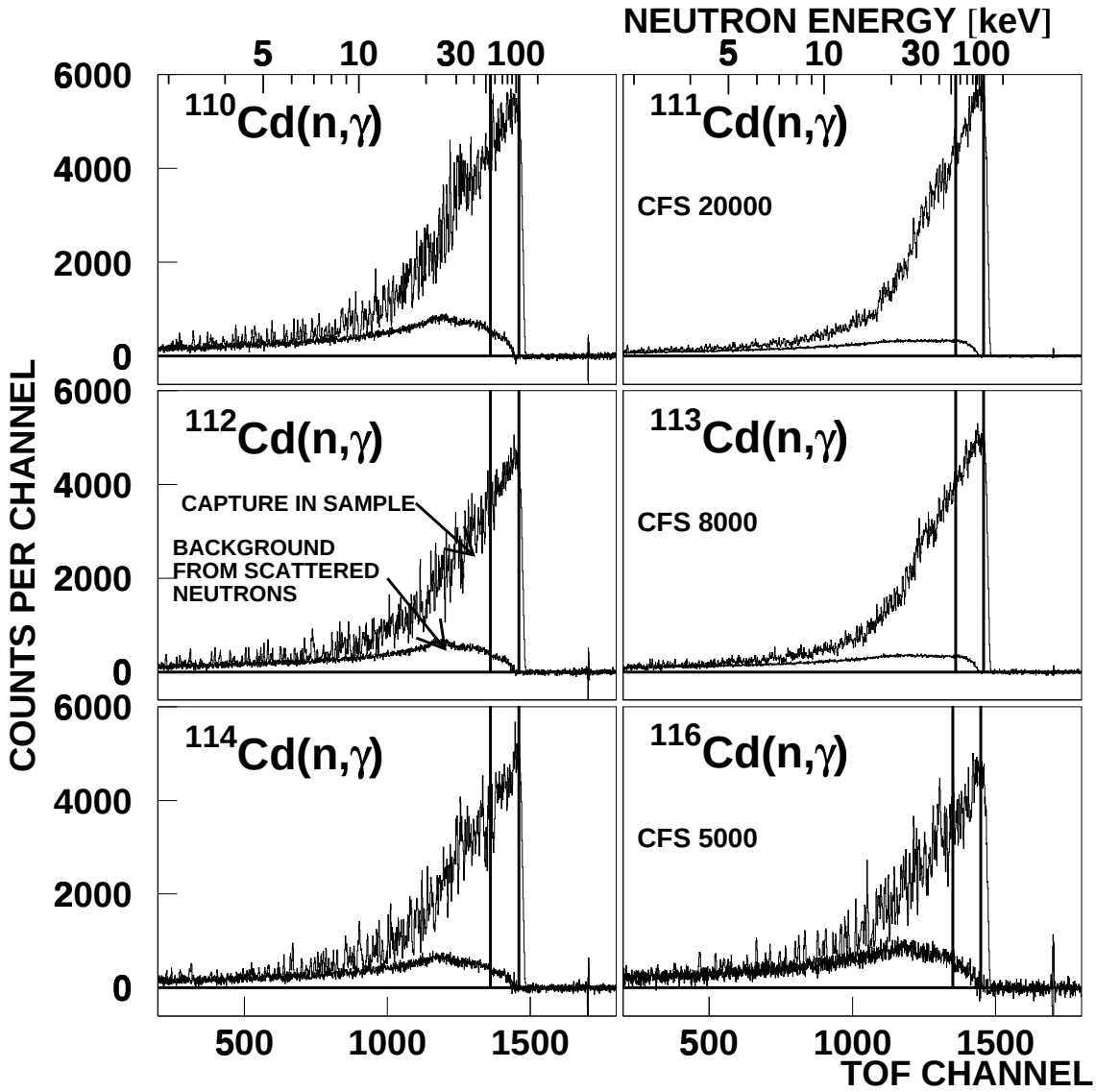

Figure 6: TOF spectra measured with the cadmium samples in run I (100 keV maximum neutron energy). The background due to sample scattered neutrons is shown separately. The region used for absolute normalization of the cross section is indicated by two vertical lines.

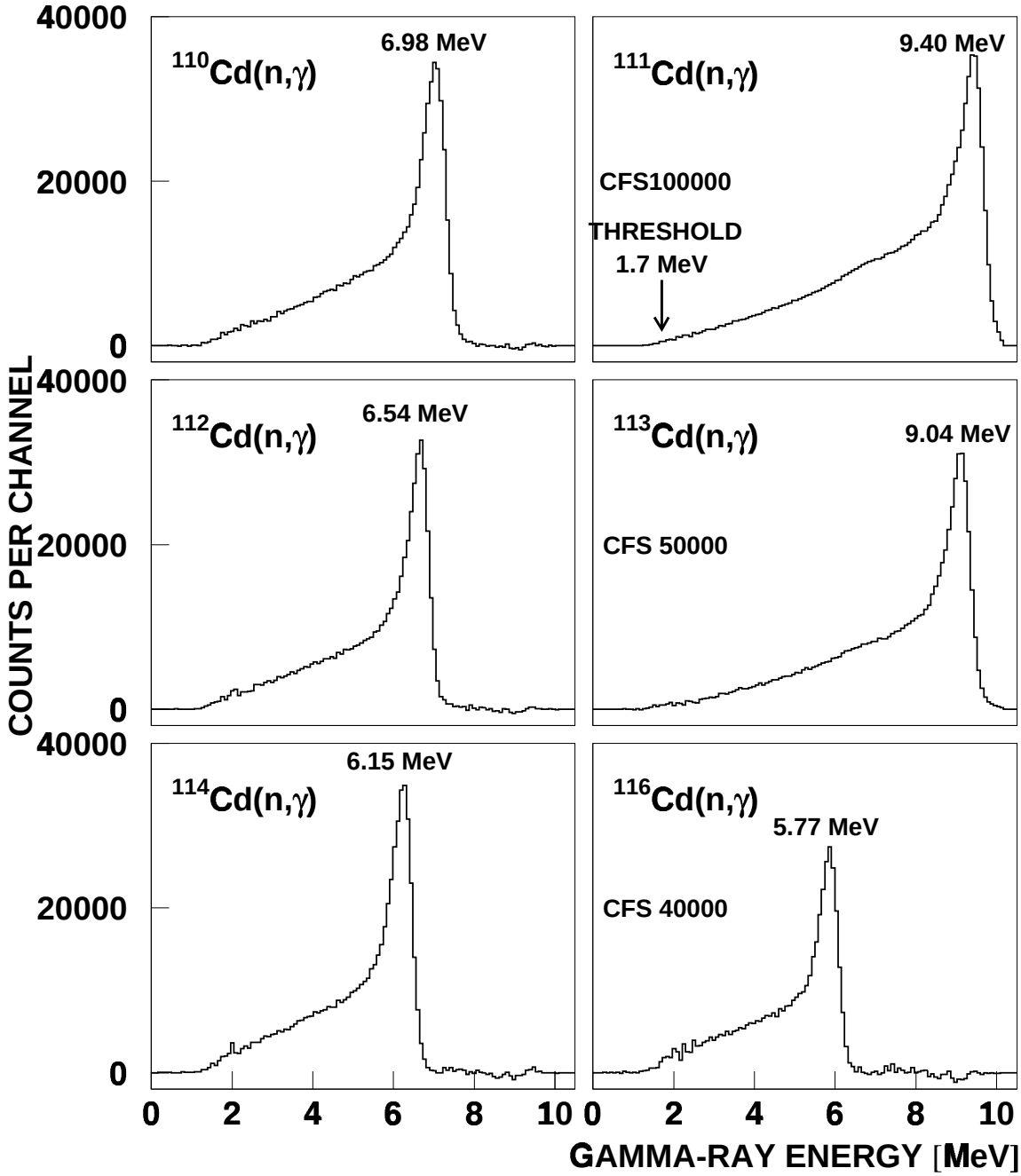

Figure 7: Sum energy spectra of all isotopes measured in run III containing events with multiplicity >2. These spectra were obtained by projection of the two–dimensional spectra in the TOF region below the maximum neutron energy as indicated by vertical lines in Fig. 6.

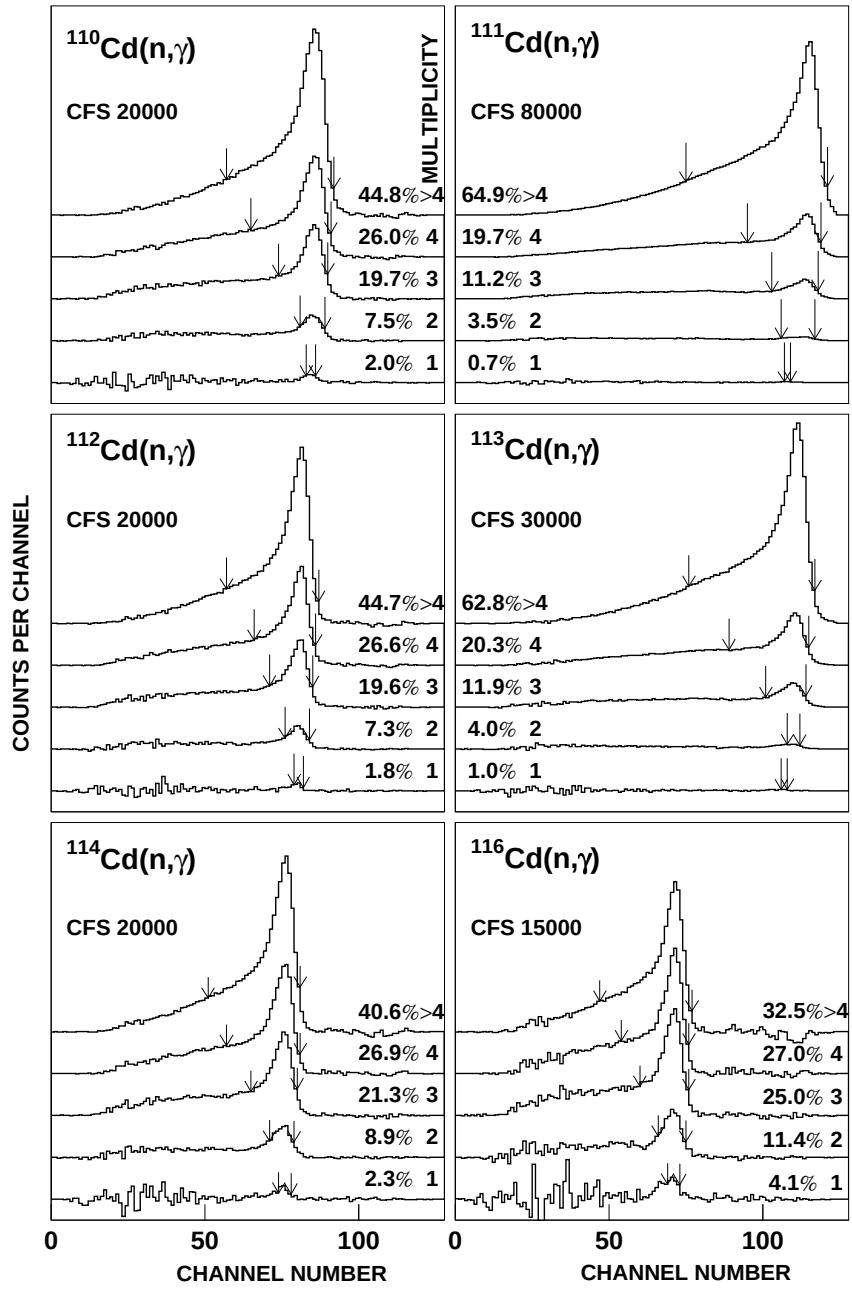

Figure 8: Sum energy spectra of all isotopes as a function of multiplicity. The regions integrated to determine the cross section shape (see TOF spectra of Fig. 6) are indicated by arrows.

The cross section ratio of isotope X relative to the gold standard is given by

$$\frac{\sigma_i(X)}{\sigma_i(Au)} = \frac{Z_i(X)}{Z_i(Au)} \frac{\Sigma Z(Au)}{\Sigma Z(X)} \frac{\Sigma E(X)}{\Sigma E(Au)} \frac{m(Au)}{m(X)} F_1 F_2. \quad (1)$$

In this expression, Z_i is the count rate of channel i in the TOF spectrum, ΣZ is the TOF rate integrated over the interval used for normalization (vertical lines in Fig. 6), ΣE is the total count rate in the sum energy spectra for all multiplicities in this TOF interval. The respective sum energy spectra are shown in Fig. 8. For all multiplicities these spectra were integrated from the threshold at 1.7 MeV beyond the binding energy, and the sum of these results, ΣE is used in Eq. 1. A full description of this procedure is given in Ref.[15]. The quantity m is the sample thickness in atoms/b. The factor F_1 $= [100 - f(Au)]/[100 - f(X)]$ corrects for the fraction of capture events f below the experimental threshold in sum energy, where X refers to the respective cadmium sample (Table 8), and F_2 is the ratio of the multiple scattering and self–shielding corrections.

The fraction of unobserved capture events, f, and the correction factor F_1 were calculated as described in Ref. [11]. The input for this calculation are the individual neutron capture cascades and their relative contributions to the total capture cross section as well as the detector efficiency for monoenergetic γ-rays in the energy range up to 10 MeV. As in the experiment on dysprosium isotopes [16] this information was derived directly from the experimental data recorded with the ADC system in Run I. From these data, only events close to the sum energy peak (see Fig. 7) were selected, which contained the full capture γ-ray cascade. This ensemble was further reduced by restricting the analysis to the TOF region with optimum signal-to-background ratio (vertical lines in Fig. 6). The correction factors F_1 were calculated as described in Ref. [11] and are quoted in Table 8. As in all previous experiments with the 4π BaF_2 detector, F_1 was found to depend linearly on the binding energy of the captured neutron.

The capture γ-ray spectra obtained from the data taken with the ADC system are shown in Fig. 9 in energy bins of 500 keV. The spectra of the even target isotopes show a hard component, well correlated with the intensity in the spectra of multiplicity 1 and 2 in Fig. 8, which increases from 9.5% in ^{110}Cd to 15.5% in ^{116}Cd. The relative intensities for multiplicities 1 and 2 suggest that these two-step cascades consist of primary transitions feeding levels close to the ground state. The pronounced peak in the spectra of the odd isotopes in the second bin reflects the energy differences of more than 500 keV between the first excited 2^+ state and the ground state (0^+) as well as between the second excited 0^+ state and the first excited state in both compound nuclei.

The correction for neutron multiple scattering and self-shielding was calculated with the SESH code [12]. Apart from the pairing energies [17], most of the input parameters were taken from Ref. [18], but were slightly modified in order to reproduce the measured total and capture cross sections. The final values are listed in Table 9 together with the calculated total cross sections. The resulting correction factors, MS(X) and F_2, are compiled in Tables 10 and 11. In general, these corrections are smaller than 5% except for the even isotopes at energies below 10 keV. However, somewhat larger corrections are required for ^{114}Cd and ^{116}Cd.

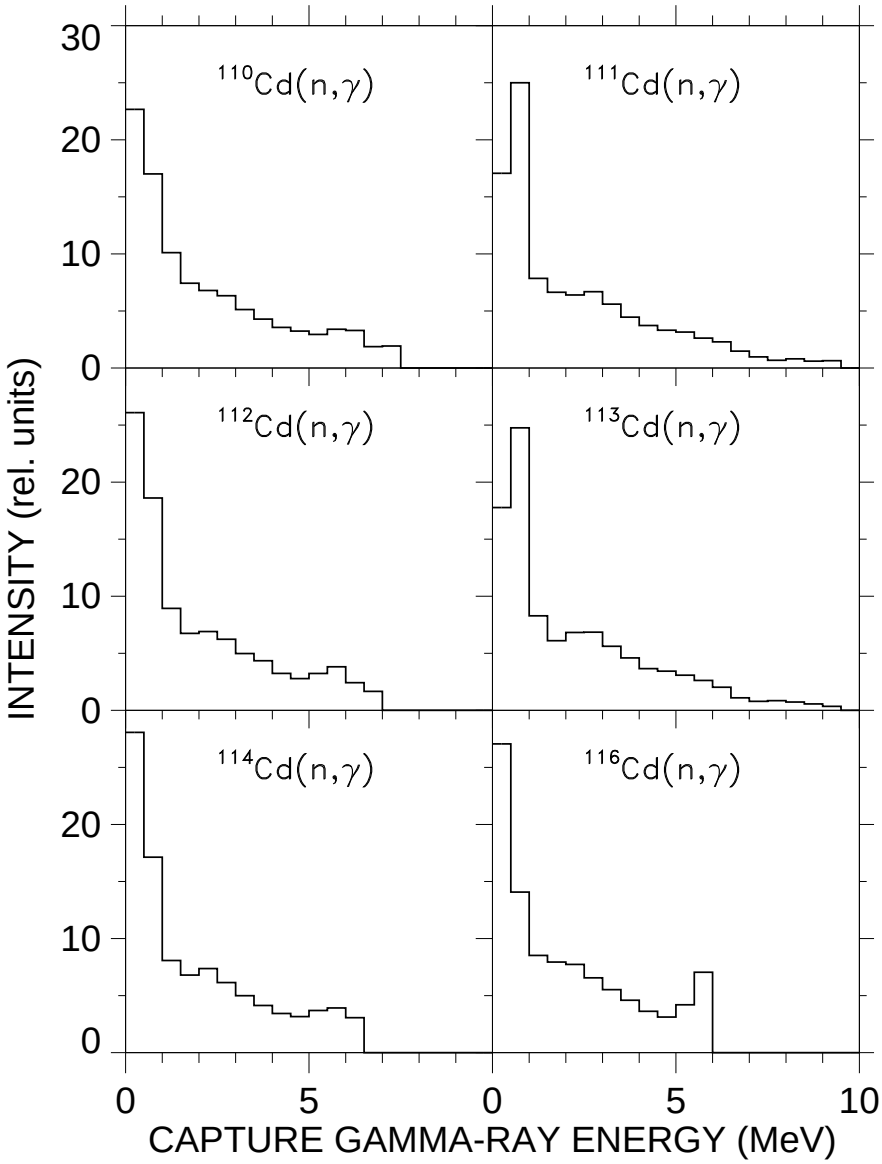

Figure 9: Capture γ-ray spectra derived from the capture cascades recorded with the ADC system. (The full resolution of 2048 channels is compressed into bins of 500 keV.)

Table 8: FRACTION OF UNDETECTED CAPTURE EVENTS, f (%), AND THE RELATED CORRECTION FACTORS F_1.[a]

	Threshold in Sum Energy (MeV)				
	1.5	1.6	1.7	1.8	2.0
f(Au)	4.99				6.94
f(^{110}Cd)	3.72				5.27
f(^{111}Cd)	1.29				1.88
f(^{112}Cd)	4.03				5.61
f(^{113}Cd)	1.41				2.06
f(^{114}Cd)	4.70				6.43
f(^{116}Cd)	5.15				7.02
F_1(^{110}Cd/Au)	0.987	0.986	0.985	0.984	0.982
F_1(^{111}Cd/Au)	0.963	0.960	0.957	0.954	0.948
F_1(^{112}Cd/Au)	0.990	0.989	0.988	0.988	0.986
F_1(^{113}Cd/Au)	0.964	0.961	0.958	0.956	0.950
F_1(^{114}Cd/Au)	0.997	0.997	0.996	0.996	0.995
F_1(^{116}Cd/Au)	1.002	1.002	1.001	1.001	1.001

[a] derived from capture cascades measured with the ADC system.

Table 9: PARAMETERS FOR THE CALCULATION OF NEUTRON SELF–SHIELDING AND MULTIPLE SCATTERING CORRECTIONS

Parameter		^{110}Cd	^{111}Cd	^{112}Cd	^{113}Cd	^{114}Cd	^{116}Cd
Nucleon Number		110	111	112	113	114	116
Binding Energy (MeV)		6.976	9.398	6.540	9.043	6.141	5.777
Pairing Energy (MeV)		1.36	2.50	1.36	2.68	1.36	1.36
Effective Temperature (K)		293	293	293	293	293	293
Nuclear Spin		0	0.5	0	0.5	0	0
Average Radiation	s	0.090	0.140	0.080	0.120	0.053	0.040
Width (eV)	p	0.060	0.100	0.040	0.050	0.040	0.035
	d	0.060	0.100	0.040	0.050	0.070	0.020
Average Level	s	155.	20.	190.	21.	235.	390.
Spacing (eV)	p[a]	51.7	8.9	63.3	9.3	78.3	130.
	d[a]	31.0	5.3	38.0	5.6	47.0	78.
Strength Function	S_0	0.44	0.50	0.3	0.6	0.3	0.05
(10^{-4})	S_1	3.0	3.2	3.2	5.0	3.5	3.2
	S_2	1.0	1.0	3.0	5.0	1.0	1.0
Nuclear Radius	s	6.28	6.24	6.20	6.18	6.14	6.10
(fm)	p	6.28	6.24	6.20	6.18	6.14	6.10
	d	6.28	6.24	6.20	6.18	6.14	6.10
		Calculated total cross sections					
3 keV		8.7	9.1	7.5	10.0	7.5	5.5
5 keV		8.0	8.4	7.2	9.2	7.1	5.6
10 keV		7.5	7.7	6.9	8.5	6.8	5.7
20 keV		7.2	7.4	6.8	8.2	6.8	6.0
40 keV		7.1	7.3	6.9	8.3	6.9	6.3
80 keV		7.2	7.3	7.1	8.6	7.2	6.7
160 keV		7.3	7.4	7.4	9.1	7.5	7.1
320 keV		7.2	7.4	7.7	9.5	7.6	7.3

[a]Calculated with SESH [12]

Table 10: CORRECTION FACTORS FOR NEUTRON SELF–SHIELDING AND MULTIPLE SCATTERING, MS

Energy Bin	MS						
(keV)	^{197}Au	^{110}Cd	^{111}Cd	^{112}Cd	^{113}Cd	^{114}Cd	^{116}Cd
3 – 5	0.994	0.873	0.979	0.893	0.996	0.846	0.841
5 – 7.5	1.016	0.943	1.001	0.938	1.007	0.899	0.865
7.5 – 10	1.028	0.967	1.008	0.956	1.011	0.919	0.879
10 – 12.5	1.033	0.979	1.014	0.968	1.013	0.932	0.892
12.5 –15	1.036	0.986	1.017	0.976	1.014	0.943	0.901

Table 10 (continued)

15 – 20	1.038	0.993	1.021	0.982	1.015	0.954	0.911
20 – 25	1.038	0.999	1.023	0.989	1.017	0.965	0.921
25 – 30	1.038	1.003	1.025	0.993	1.018	0.974	0.929
30 – 40	1.037	1.008	1.027	0.999	1.019	0.983	0.940
40 – 50	1.036	1.013	1.028	1.003	1.020	0.992	0.950
50 – 60	1.035	1.016	1.029	1.006	1.021	0.999	0.956
60 – 80	1.034	1.019	1.029	1.009	1.022	1.006	0.964
80 – 100	1.032	1.021	1.030	1.011	1.023	1.010	0.971
100 – 120	1.031	1.022	1.030	1.013	1.023	1.013	0.977
120 – 150	1.030	1.023	1.031	1.016	1.024	1.016	0.983
150 – 175	1.029	1.023	1.031	1.018	1.025	1.018	0.989
175 – 200	1.028	1.024	1.031	1.019	1.025	1.020	0.994
200 – 225	1.027	1.024	1.031	1.021	1.026	1.021	0.998
Uncertainty (%)	0.3	0.4	0.2	0.5	0.2	0.6	0.9

Table 11: CORRECTION FACTORS FOR THE CROSS SECTION RATIOS, F_2 = MS(Au)/MS(X)

Energy Bin	F_2					
(keV)	^{110}Cd/Au	^{111}Cd/Au	^{112}Cd/Au	^{113}Cd/Au	^{114}Cd/Au	^{116}Cd/Au
3 – 5	1.139	1.015	1.113	0.998	1.175	1.182
5 – 7.5	1.077	1.015	1.083	1.009	1.130	1.175
7.5– 10	1.063	1.020	1.075	1.017	1.119	1.170
10 – 12.5	1.055	1.019	1.067	1.020	1.108	1.158
12.5 – 15	1.051	1.019	1.061	1.022	1.099	1.150
15 – 20	1.045	1.017	1.057	1.023	1.088	1.139
20 – 25	1.039	1.015	1.050	1.021	1.076	1.127
25 – 30	1.035	1.013	1.045	1.020	1.066	1.117
30 – 40	1.029	1.010	1.038	1.018	1.055	1.103
40 – 50	1.023	1.008	1.033	1.016	1.044	1.091
50 – 60	1.019	1.006	1.029	1.014	1.036	1.083
60 – 80	1.015	1.005	1.025	1.012	1.028	1.073
80 – 100	1.011	1.002	1.021	1.009	1.022	1.063
100 – 120	1.009	1.001	1.018	1.008	1.018	1.055
120 – 150	1.007	0.999	1.014	1.006	1.014	1.048
150 – 175	1.006	0.998	1.011	1.004	1.011	1.040
175 – 200	1.004	0.997	1.009	1.003	1.008	1.034
200 – 225	1.003	0.996	1.006	1.001	1.006	1.029
Uncertainty (%)	0.5	0.4	0.6	0.4	0.7	0.9

4 RESULTS FOR THE NEUTRON CAPTURE CROSS SECTIONS

The measured neutron capture cross section ratios of the investigated Cd isotopes, and of ^{197}Au are listed in Tables 12 to 17 together with the respective statistical uncertainties. The data are given for all runs and for the two evaluation methods discussed in Sec. 3. The last column in each table contains the weighted average, the weight being determined by the inverse of the squared statistical uncertainties. Since the cross section ratios depend weakly on energy, the averages for the energy interval from 30 to 80 keV are also included for a better comparison of the individual results. The data are free of systematic differences with respect to different runs or evaluations. This is important as they were obtained with different data acquisition modes and different neutron spectra. However, the results for ^{113}Cd differ on average by 2.3 standard deviations from the weighted mean. Though not completely excluded by statistics, this large deviation seems to reflect the problems in subtracting the background due to scattered neutrons, which is crucial for isotopes with high binding energies (see Sec. 3).

As in the previous measurements with the 4π BaF_2 detector [8, 9, 19], the final cross section ratios were adopted from evaluation 2. The respective mean values are compiled for all runs in Table 18 together with the statistical, systematic, and total uncertainties. The energy bins are sufficiently fine to avoid systematic uncertainties in the calculation of the Maxwellian averaged cross sections (Sec. 6). In the energy range from 15 to 100 keV statistical uncertainties of less than 1.2% could be obtained for all investigated cross sections. The systematic uncertainties range between 0.7 and 1.6%.

The experimental ratios were converted into absolute cross sections using the gold data of Macklin [20] after normalization by a factor of 0.989 to the absolute value of Ratynski and Käppeler [21] (Table 19). The uncertainties of the resulting values can be obtained by adding the 1.5% uncertainty of the reference cross section to the uncertainties of the respective cross section ratios.

In Figs. 10 to 12 the present results are compared to previous data of Musgrove *et al.* [2, 3] which were corrected according to Ref.[4]. The 12 - 16% uncertainties of the older values could be improved by almost an order of magnitude. In general, the present results are systematically lower, the differences reaching up to 40%.

Table 12: $\sigma(^{110}\mathrm{Cd})/\sigma(^{197}\mathrm{Au})$ AND STATISTICAL UNCERTAINTIES IN (%)

Energy Bin (keV)	Run I		Run II		Run III		Average	
evaluation 1								
3 – 5	0.3746	7.9	0.3730	7.5	0.2591	15.	0.3604	5.1
5 – 7.5	0.3193	5.0	0.3094	4.7	0.3156	6.9	0.3144	3.1
7.5 – 10	0.4686	3.3	0.4538	3.6	0.4922	5.1	0.4674	2.2
10 – 12.5	0.4115	2.6	0.4072	2.8	0.4004	3.8	0.4076	1.7
12.5 – 15	0.5062	2.1	0.4979	2.3	0.4916	3.1	0.5003	1.4
15 – 20	0.5217	1.3	0.5223	1.4	0.5148	1.8	0.5203	0.8
20 – 25	0.4901	1.2	0.4918	1.3	0.4846	1.6	0.4894	0.8
25 – 30	0.4350	1.0	0.4336	1.1	0.4172	1.3	0.4300	0.7
30 – 40	0.4299	0.8	0.4288	0.9	0.4272	0.9	0.4287	0.5
40 – 50	0.4109	0.9	0.4122	0.9	0.4034	1.0	0.4092	0.5
50 – 60	0.4143	0.8	0.4178	0.9	0.4117	1.0	0.4148	0.5
60 – 80	0.3885	0.7	0.3880	0.8	0.3882	0.8	0.3882	0.4
80 – 100	0.3805	0.8	0.3812	0.8	0.3725	0.8	0.3782	0.5
100 – 120	0.3658	0.8	0.3649	0.9	0.3649	0.8	0.3652	0.5
120 – 150	–	–	–	–	0.3567	0.7	0.3567	0.7
150 – 175	–	–	–	–	0.3580	0.8	0.3580	0.8
175 – 200	–	–	–	–	0.3537	0.8	0.3537	0.8
200 – 225	–	–	–	–	0.3641	1.1	0.3641	1.1
30 – 80	0.4109	0.6	0.4117	0.7	0.4076	0.6	0.4099	0.4
evaluation 2								
3 – 5	0.3680	5.8	0.3672	5.5	0.2591	10.	0.3536	3.7
5 – 7.5	0.3206	3.7	0.3099	3.3	0.3092	5.0	0.3137	2.2
7.5 – 10	0.4650	2.5	0.4403	2.7	0.4505	3.7	0.4530	1.6
10 – 12.5	0.4017	2.0	0.3924	2.1	0.3979	2.9	0.3975	1.3
12.5 – 15	0.5085	1.6	0.4970	1.8	0.4942	2.4	0.5014	1.1
15 – 20	0.5190	1.1	0.5186	1.1	0.5252	1.4	0.5203	0.7
20 – 25	0.4927	1.0	0.4913	1.0	0.4878	1.2	0.4910	0.6
25 – 30	0.4410	0.8	0.4370	0.9	0.4270	1.0	0.4360	0.5
30 – 40	0.4308	0.7	0.4259	0.7	0.4286	0.8	0.4285	0.4
40 – 50	0.4107	0.7	0.4110	0.7	0.4071	0.8	0.4098	0.4
50 – 60	0.4120	0.7	0.4139	0.7	0.4135	0.8	0.4131	0.4
60 – 80	0.3851	0.6	0.3841	0.6	0.3885	0.7	0.3857	0.4
80 – 100	0.3772	0.6	0.3769	0.7	0.3724	0.7	0.3757	0.4
100 – 120	0.3633	0.7	0.3597	0.8	0.3651	0.7	0.3629	0.4
120 – 150	–	–	–	–	0.3559	0.6	0.3559	0.6
150 – 175	–	–	–	–	0.3599	0.7	0.3599	0.7
175 – 200	–	–	–	–	0.3535	0.7	0.3535	0.7
200 – 225	–	–	–	–	0.3656	1.0	0.3656	1.0
30 – 80	0.4097	0.5	0.4087	0.5	0.4094	0.5	0.4093	0.3

Table 13: $\sigma(^{111}\mathrm{Cd})/\sigma(^{197}\mathrm{Au})$ AND STATISTICAL UNCERTAINTIES IN (%)

Energy Bin (keV)	Run I		Run II		Run III		Average	
evaluation 1								
3 – 5	0.7288	6.8	0.6149	6.8	0.8363	10.	0.7030	4.4
5 – 7.5	0.7999	3.9	0.8712	3.5	0.8912	5.4	0.8487	2.4
7.5 – 10	0.9557	3.0	0.9953	3.2	1.0506	4.7	0.9876	2.0
10 – 12.5	1.0834	2.2	1.0927	2.3	1.0222	3.2	1.0750	1.4
12.5 – 15	1.1921	1.9	1.2437	2.1	1.1885	2.8	1.2101	1.2
15 – 20	1.3021	1.2	1.3246	1.2	1.2347	1.6	1.2959	0.8
20 – 25	1.5381	1.0	1.5560	1.1	1.4678	1.4	1.5284	0.6
25 – 30	1.5373	0.8	1.5374	0.9	1.4590	1.1	1.5177	0.5
30 – 40	1.5322	0.7	1.5345	0.7	1.4806	0.8	1.5181	0.4
40 – 50	1.5066	0.7	1.5039	0.7	1.4444	0.8	1.4877	0.4
50 – 60	1.5005	0.7	1.4887	0.7	1.4816	0.8	1.4913	0.4
60 – 80	1.4360	0.6	1.4297	0.6	1.4101	0.7	1.4260	0.4
80 – 100	1.4431	0.6	1.4389	0.7	1.4142	0.7	1.4325	0.4
100 – 120	1.3723	0.7	1.3649	0.8	1.3530	0.7	1.3633	0.4
120 – 150	–	–	–	–	1.2838	0.6	1.2838	0.6
150 – 175	–	–	–	–	1.2267	0.6	1.2267	0.6
175 – 200	–	–	–	–	1.1981	0.7	1.1981	0.7
200 – 225	–	–	–	–	1.2156	0.9	1.2156	0.9
30 – 80	1.4938	0.5	1.4892	0.5	1.4542	0.5	1.4791	0.3
evaluation 2								
3 – 5	0.7477	4.9	0.6461	5.0	0.7129	7.3	0.7008	3.1
5 – 7.5	0.8304	2.8	0.8390	2.6	0.8509	3.9	0.8381	1.7
7.5 – 10	1.0050	2.2	0.9856	2.4	1.0162	3.4	0.9999	1.5
10 – 12.5	1.0875	1.6	1.0763	1.8	1.0667	2.5	1.0794	1.1
12.5 – 15	1.2286	1.4	1.2282	1.6	1.2249	2.2	1.2277	1.0
15 – 20	1.3243	0.9	1.3324	1.0	1.3006	1.3	1.3221	0.6
20 – 25	1.5245	0.8	1.5280	0.9	1.4834	1.1	1.5162	0.5
25 – 30	1.5090	0.7	1.5089	0.7	1.4731	0.9	1.5000	0.4
30 – 40	1.5193	0.5	1.5209	0.6	1.5040	0.6	1.5156	0.3
40 – 50	1.4932	0.6	1.4854	0.6	1.4575	0.7	1.4807	0.3
50 – 60	1.4902	0.5	1.4803	0.6	1.4925	0.7	1.4874	0.3
60 – 80	1.4259	0.5	1.4170	0.5	1.4258	0.6	1.4230	0.3
80 – 100	1.4168	0.5	1.4208	0.5	1.4109	0.6	1.4164	0.3
100 – 120	1.3487	0.5	1.3425	0.6	1.3527	0.6	1.3484	0.3
120 – 150	–	–	–	–	1.2793	0.5	1.2793	0.5
150 – 175	–	–	–	–	1.2210	0.6	1.2210	0.6
175 – 200	–	–	–	–	1.1904	0.6	1.1904	0.6
200 – 225	–	–	–	–	1.2071	0.8	1.2071	0.8
30 – 80	1.4822	0.4	1.4759	0.4	1.4700	0.4	1.4760	0.2

Table 14: $\sigma(^{112}\mathrm{Cd})/\sigma(^{197}\mathrm{Au})$ AND STATISTICAL UNCERTAINTIES IN (%)

Energy Bin (keV)	Run I		Run II		Run III		Average	
evaluation 1								
3 – 5	0.2686	8.7	0.3112	7.3	0.2695	13.	0.2897	5.2
5 – 7.5	0.2788	4.9	0.2943	4.3	0.2947	6.7	0.2888	2.9
7.5 – 10	0.3435	3.5	0.3513	3.7	0.3721	5.4	0.3517	2.3
10 – 12.5	0.3660	2.5	0.3792	2.6	0.3652	3.7	0.3710	1.6
12.5 – 15	0.4466	2.0	0.4662	2.2	0.4709	3.0	0.4586	1.3
15 – 20	0.3527	1.4	0.3574	1.5	0.3386	2.0	0.3514	0.9
20 – 25	0.3935	1.2	0.3922	1.3	0.3989	1.6	0.3943	0.8
25 – 30	0.3210	1.1	0.3252	1.2	0.3085	1.4	0.3194	0.7
30 – 40	0.3249	0.9	0.3278	0.9	0.3236	1.0	0.3255	0.5
40 – 50	0.3191	0.9	0.3221	1.0	0.3122	1.0	0.3182	0.6
50 – 60	0.3233	0.9	0.3256	0.9	0.3224	1.0	0.3239	0.5
60 – 80	0.3178	0.8	0.3179	0.8	0.3156	0.9	0.3172	0.5
80 – 100	0.3160	0.8	0.3201	0.8	0.3097	0.9	0.3154	0.5
100 – 120	0.2978	0.9	0.2990	1.0	0.2959	0.9	0.2975	0.5
120 – 150	–	–	–	–	0.2928	0.8	0.2928	0.8
150 – 175	–	–	–	–	0.3001	0.8	0.3001	0.8
175 – 200	–	–	–	–	0.3099	0.9	0.3099	0.9
200 – 225	–	–	–	–	0.3095	1.2	0.3095	1.2
30 – 80	0.3213	0.7	0.3234	0.7	0.3185	0.6	0.3208	0.4
evaluation 2								
3 – 5	0.2776	6.0	0.3108	5.4	0.2707	9.1	0.2920	3.7
5 – 7.5	0.2892	3.5	0.2851	3.2	0.2951	4.8	0.2885	2.1
7.5 – 10	0.3484	2.6	0.3418	2.8	0.3613	3.9	0.3484	1.7
10 – 12.5	0.3543	1.9	0.3740	2.0	0.3630	2.9	0.3635	1.3
12.5 – 15	0.4490	1.6	0.4523	1.8	0.4620	2.3	0.4529	1.1
15 – 20	0.3452	1.1	0.3458	1.2	0.3364	1.6	0.3435	0.7
20 – 25	0.3992	1.0	0.3925	1.1	0.4042	1.3	0.3981	0.6
25 – 30	0.3275	0.9	0.3261	1.0	0.3185	1.1	0.3248	0.6
30 – 40	0.3247	0.7	0.3246	0.8	0.3252	0.8	0.3248	0.4
40 – 50	0.3201	0.7	0.3196	0.8	0.3165	0.9	0.3190	0.5
50 – 60	0.3225	0.7	0.3223	0.7	0.3248	0.9	0.3230	0.4
60 – 80	0.3160	0.6	0.3121	0.7	0.3167	0.7	0.3149	0.4
80 – 100	0.3142	0.6	0.3145	0.7	0.3104	0.7	0.3132	0.4
100 – 120	0.2961	0.7	0.2940	0.8	0.2968	0.7	0.2958	0.4
120 – 150	–	–	–	–	0.2924	0.7	0.2924	0.7
150 – 175	–	–	–	–	0.3025	0.7	0.3025	0.7
175 – 200	–	–	–	–	0.3119	0.8	0.3119	0.8
200 – 225	–	–	–	–	0.3112	1.0	0.3112	1.0
30 – 80	0.3208	0.5	0.3197	0.5	0.3208	0.5	0.3204	0.3

Table 15: $\sigma(^{113}\mathrm{Cd})/\sigma(^{197}\mathrm{Au})$ AND STATISTICAL UNCERTAINTIES IN (%)

Energy Bin (keV)	Run I		Run II		Run III		Average	
evaluation 1								
3 – 5	0.4270	14.	0.7338	9.6	0.2387	36.	0.6163	8.0
5 – 7.5	0.7647	5.3	0.9805	4.6	0.5939	9.1	0.8503	3.3
7.5 – 10	1.0136	3.7	1.1501	4.0	0.9061	6.3	1.0506	2.5
10 – 12.5	1.0325	2.7	1.1524	2.9	0.8546	4.4	1.0485	1.8
12.5 – 15	1.0727	2.3	1.1948	2.6	0.9954	3.6	1.1027	1.5
15 – 20	1.2804	1.3	1.3364	1.5	1.1949	1.9	1.2824	0.9
20 – 25	1.3780	1.1	1.4670	1.2	1.3262	1.6	1.3977	0.7
25 – 30	1.3442	0.9	1.3984	1.0	1.3035	1.2	1.3525	0.6
30 – 40	1.2814	0.8	1.3056	0.8	1.2650	0.9	1.2848	0.5
40 – 50	1.3259	0.8	1.3458	0.8	1.3182	0.9	1.3302	0.5
50 – 60	1.2503	0.8	1.2669	0.8	1.2885	0.9	1.2664	0.5
60 – 80	1.1988	0.7	1.2154	0.7	1.2367	0.7	1.2155	0.4
80 – 100	1.1877	0.7	1.2026	0.7	1.2109	0.7	1.1997	0.4
100 – 120	1.1588	0.7	1.1543	0.9	1.1616	0.7	1.1586	0.4
120 – 150	–	–	–	–	1.0910	0.7	1.0910	0.7
150 – 175	–	–	–	–	1.0532	0.7	1.0532	0.7
175 – 200	–	–	–	–	1.0291	0.8	1.0291	0.8
200 – 225	–	–	–	–	1.0271	1.1	1.0271	1.1
30 – 80	1.2641	0.6	1.2834	0.6	1.2771	0.5	1.2751	0.3
evaluation 2								
3 – 5	0.5288	8.4	0.6828	7.4	0.3162	20.	0.5949	5.5
5 – 7.5	0.8036	3.8	0.9029	3.5	0.6455	6.4	0.8279	2.4
7.5 – 10	1.0038	2.8	1.0773	3.1	0.9565	4.5	1.0227	1.9
10 – 12.5	0.9914	2.1	1.0788	2.3	0.9188	3.3	1.0107	1.4
12.5 – 15	1.0855	1.8	1.1350	2.0	1.0528	2.7	1.0964	1.2
15 – 20	1.2770	1.1	1.3233	1.2	1.2572	1.5	1.2889	0.7
20 – 25	1.3553	0.9	1.4129	1.0	1.3448	1.2	1.3724	0.6
25 – 30	1.3147	0.8	1.3645	0.9	1.3134	1.0	1.3310	0.5
30 – 40	1.2644	0.6	1.2876	0.7	1.2798	0.7	1.2761	0.4
40 – 50	1.3049	0.6	1.3234	0.7	1.3175	0.7	1.3144	0.4
50 – 60	1.2381	0.6	1.2573	0.7	1.2879	0.8	1.2572	0.4
60 – 80	1.1887	0.5	1.2086	0.6	1.2418	0.6	1.2093	0.3
80 – 100	1.1701	0.5	1.1961	0.6	1.2033	0.6	1.1882	0.3
100 – 120	1.1396	0.6	1.1419	0.7	1.1606	0.6	1.1473	0.4
120 – 150	–	–	–	–	1.0911	0.6	1.0911	0.6
150 – 175	–	–	–	–	1.0527	0.6	1.0527	0.6
175 – 200	–	–	–	–	1.0298	0.7	1.0298	0.7
200 – 225	–	–	–	–	1.0241	1.0	1.0241	1.0
30 – 80	1.2490	0.4	1.2692	0.4	1.2818	0.4	1.2667	0.2

Table 16: $\sigma(^{114}\mathrm{Cd})/\sigma(^{197}\mathrm{Au})$ AND STATISTICAL UNCERTAINTIES IN (%)

Energy Bin (keV)	Run I		Run II		Run III		Average	
evaluation 1								
3 – 5	0.1584	12.	0.1722	10.	0.1906	15.	0.1718	7.0
5 – 7.5	0.2202	5.3	0.2333	4.6	0.2221	7.0	0.2266	3.1
7.5 – 10	0.2399	4.0	0.2534	4.0	0.2785	5.6	0.2532	2.5
10 – 12.5	0.2524	2.9	0.2743	2.9	0.2526	4.0	0.2612	1.8
12.5 – 15	0.2563	2.5	0.2567	2.7	0.2721	3.4	0.2599	1.6
15 – 20	0.2451	1.7	0.2486	1.7	0.2472	2.1	0.2469	1.0
20 – 25	0.2598	1.4	0.2548	1.5	0.2562	1.8	0.2571	0.9
25 – 30	0.2416	1.3	0.2401	1.3	0.2315	1.5	0.2383	0.8
30 – 40	0.2408	1.1	0.2407	1.1	0.2350	1.1	0.2389	0.6
40 – 50	0.2243	1.1	0.2253	1.1	0.2196	1.1	0.2232	0.6
50 – 60	0.2063	1.1	0.2070	1.1	0.2048	1.2	0.2061	0.6
60 – 80	0.2149	1.0	0.2161	1.0	0.2148	1.0	0.2153	0.6
80 – 100	0.2118	1.0	0.2129	1.0	0.2092	1.0	0.2113	0.6
100 – 120	0.2159	1.0	0.2154	1.1	0.2147	1.0	0.2153	0.6
120 – 150	–	–	–	–	0.2137	0.9	0.2137	0.9
150 – 175	–	–	–	–	0.2157	0.9	0.2157	0.9
175 – 200	–	–	–	–	0.2109	1.0	0.2109	1.0
200 – 225	–	–	–	–	0.2197	1.2	0.2197	1.2
30 – 80	0.2216	0.9	0.2223	0.9	0.2185	0.7	0.2206	0.5
evaluation 2								
3 – 5	0.1541	9.0	0.1585	8.3	0.1437	13.	0.1542	5.6
5 – 7.5	0.2212	3.9	0.2202	3.5	0.1972	5.6	0.2165	2.4
7.5 – 10	0.2519	2.9	0.2520	3.1	0.2540	4.3	0.2524	1.9
10 – 12.5	0.2435	2.2	0.2585	2.3	0.2549	3.1	0.2516	1.4
12.5 – 15	0.2546	1.9	0.2477	2.1	0.2644	2.7	0.2544	1.3
15 – 20	0.2397	1.3	0.2395	1.4	0.2419	1.7	0.2401	0.8
20 – 25	0.2614	1.1	0.2547	1.2	0.2559	1.4	0.2577	0.7
25 – 30	0.2426	1.0	0.2394	1.1	0.2366	1.2	0.2399	0.6
30 – 40	0.2404	0.8	0.2376	0.8	0.2386	0.9	0.2389	0.5
40 – 50	0.2257	0.8	0.2238	0.9	0.2218	0.9	0.2239	0.5
50 – 60	0.2057	0.8	0.2047	0.9	0.2067	1.0	0.2056	0.5
60 – 80	0.2144	0.7	0.2140	0.7	0.2173	0.8	0.2151	0.4
80 – 100	0.2100	0.8	0.2109	0.8	0.2104	0.8	0.2104	0.5
100 – 120	0.2152	0.8	0.2135	0.9	0.2163	0.8	0.2151	0.5
120 – 150	–	–	–	–	0.2142	0.7	0.2142	0.7
150 – 175	–	–	–	–	0.2170	0.8	0.2170	0.8
175 – 200	–	–	–	–	0.2129	0.8	0.2129	0.8
200 – 225	–	–	–	–	0.2228	1.1	0.2228	1.1
30 – 80	0.2216	0.6	0.2200	0.6	0.2211	0.6	0.2209	0.3

Table 17: $\sigma(^{116}\mathrm{Cd})/\sigma(^{197}\mathrm{Au})$ AND STATISTICAL UNCERTAINTIES IN (%)

Energy Bin (keV)	Run I		Run II		Run III		Average	
evaluation 1								
3 – 5	0.1384	16.	0.0897	19.	0.1393	19.	0.1248	10.
5 – 7.5	0.1170	10.	0.1110	8.9	0.1164	12.	0.1142	5.9
7.5 – 10	0.1249	7.8	0.1323	7.0	0.1285	10.	0.1289	4.6
10 – 12.5	0.1447	5.0	0.1494	4.6	0.1438	6.1	0.1464	3.0
12.5 – 15	0.1386	4.4	0.1383	4.4	0.1467	5.3	0.1406	2.7
15 – 20	0.1696	2.4	0.1700	2.4	0.1613	2.9	0.1676	1.5
20 – 25	0.1541	2.2	0.1526	2.3	0.1500	2.6	0.1525	1.4
25 – 30	0.1467	1.9	0.1450	2.0	0.1368	2.2	0.1432	1.2
30 – 40	0.1320	1.6	0.1302	1.7	0.1255	1.7	0.1293	1.0
40 – 50	0.1303	1.6	0.1288	1.7	0.1207	1.7	0.1267	1.0
50 – 60	0.1328	1.6	0.1308	1.6	0.1264	1.7	0.1301	0.9
60 – 80	0.1257	1.5	0.1235	1.6	0.1187	1.5	0.1226	0.9
80 – 100	0.1319	1.5	0.1324	1.5	0.1291	1.4	0.1310	0.9
100 – 120	0.1233	1.5	0.1237	1.7	0.1192	1.5	0.1219	0.9
120 – 150	–	–	–	–	0.1274	1.3	0.1274	1.3
150 – 175	–	–	–	–	0.1294	1.3	0.1294	1.3
175 – 200	–	–	–	–	0.1337	1.3	0.1337	1.3
200 – 225	–	–	–	–	0.1366	1.7	0.1366	1.7
30 – 80	0.1302	1.3	0.1283	1.4	0.1228	1.1	0.1265	0.7
evaluation 2								
3 – 5	0.1194	13.	0.0965	14.	0.1159	16.	0.1103	8.3
5 – 7.5	0.0945	9.7	0.0995	7.4	0.0963	11.	0.0973	5.2
7.5 – 10	0.1277	5.8	0.1334	5.4	0.1232	7.7	0.1292	3.5
10 – 12.5	0.1294	4.1	0.1400	3.8	0.1391	5.0	0.1361	2.4
12.5 – 15	0.1373	3.4	0.1345	3.5	0.1421	4.3	0.1374	2.1
15 – 20	0.1639	1.9	0.1608	2.0	0.1607	2.4	0.1620	1.2
20 – 25	0.1546	1.7	0.1488	1.8	0.1486	2.1	0.1510	1.1
25 – 30	0.1480	1.4	0.1431	1.5	0.1402	1.7	0.1443	0.9
30 – 40	0.1303	1.2	0.1278	1.3	0.1269	1.4	0.1285	0.7
40 – 50	0.1318	1.2	0.1284	1.3	0.1229	1.4	0.1282	0.8
50 – 60	0.1336	1.2	0.1290	1.3	0.1286	1.4	0.1306	0.7
60 – 80	0.1246	1.1	0.1215	1.2	0.1214	1.2	0.1226	0.7
80 – 100	0.1329	1.1	0.1317	1.1	0.1303	1.2	0.1317	0.7
100 – 120	0.1248	1.1	0.1223	1.3	0.1208	1.2	0.1228	0.7
120 – 150	–	–	–	–	0.1286	1.1	0.1286	1.1
150 – 175	–	–	–	–	0.1315	1.1	0.1315	1.1
175 – 200	–	–	–	–	0.1361	1.1	0.1361	1.1
200 – 225	–	–	–	–	0.1398	1.4	0.1398	1.4
30 – 80	0.1301	0.9	0.1267	1.0	0.1250	0.9	0.1273	0.5

Table 18: FINAL NEUTRON CAPTURE CROSS SECTION RATIOS OF ^{110}Cd, ^{111}Cd, ^{112}Cd, ^{113}Cd ^{114}Cd, AND ^{116}Cd RELATIVE TO ^{197}Au

Energy Bin[a]	$\frac{\sigma(^{110}Cd)}{\sigma(^{197}Au)}$	Uncertainty (%)			$\frac{\sigma(^{111}Cd)}{\sigma(^{197}Au)}$	Uncertainty (%)			$\frac{\sigma(^{112}Cd)}{\sigma(^{197}Au)}$	Uncertainty (%)		
(keV)		stat	sys	tot		stat	sys	tot		stat	sys	tot
3 – 5	0.3536	3.7	0.7	3.8	0.7008	3.1	1.6	3.5	0.2920	3.7	0.8	3.8
5 – 7.5	0.3137	2.2	0.7	2.3	0.8381	1.7	1.6	2.3	0.2885	2.1	0.8	2.2
7.5 – 10	0.4530	1.6	0.7	1.7	0.9999	1.5	1.6	2.2	0.3484	1.7	0.8	1.9
10 – 12.5	0.3975	1.3	0.7	1.5	1.0794	1.1	1.6	1.9	0.3635	1.3	0.8	1.5
12.5 – 15	0.5014	1.1	0.7	1.3	1.2277	1.0	1.6	1.9	0.4529	1.1	0.8	1.4
15 – 20	0.5203	0.7	0.7	1.0	1.3221	0.6	1.6	1.7	0.3435	0.7	0.8	1.1
20 – 25	0.4910	0.6	0.7	0.9	1.5162	0.5	1.6	1.7	0.3981	0.6	0.8	1.0
25 – 30	0.4360	0.5	0.7	0.9	1.5000	0.4	1.6	1.6	0.3248	0.6	0.8	1.0
30 – 40	0.4285	0.4	0.7	0.8	1.5156	0.3	1.6	1.6	0.3248	0.4	0.8	0.9
40 – 50	0.4098	0.4	0.7	0.8	1.4807	0.3	1.6	1.6	0.3190	0.5	0.8	0.9
50 – 60	0.4131	0.4	0.7	0.8	1.4874	0.3	1.6	1.6	0.3230	0.4	0.8	0.9
60 – 80	0.3857	0.4	0.7	0.8	1.4230	0.3	1.6	1.6	0.3149	0.4	0.8	0.9
80 – 100	0.3757	0.4	0.7	0.8	1.4164	0.3	1.6	1.6	0.3132	0.4	0.8	0.9
100 – 120	0.3629	0.4	0.7	0.8	1.3484	0.3	1.6	1.6	0.2958	0.4	0.8	0.9
120 – 150	0.3559	0.6	0.7	0.9	1.2793	0.5	1.6	1.7	0.2924	0.7	0.8	1.1
150 – 175	0.3599	0.7	0.7	1.0	1.2210	0.6	1.6	1.7	0.3025	0.7	0.8	1.1
175 – 200	0.3535	0.7	0.7	1.0	1.1904	0.6	1.6	1.7	0.3119	0.8	0.8	1.1
200 – 225	0.3656	1.0	0.7	1.2	1.2071	0.8	1.6	1.8	0.3112	1.0	0.8	1.3

Energy Bin[a]	$\frac{\sigma(^{113}Cd)}{\sigma(^{197}Au)}$	Uncertainty (%)			$\frac{\sigma(^{114}Cd)}{\sigma(^{197}Au)}$	Uncertainty (%)			$\frac{\sigma(^{116}Cd)}{\sigma(^{197}Au)}$	Uncertainty (%)		
(keV)		stat	sys	tot		stat	sys	tot		stat	sys	tot
3 – 5	0.5949	5.5	1.6	5.7	0.1542	5.6	0.9	5.7	0.1103	8.3	1.1	8.4
5 – 7.5	0.8279	2.4	1.6	2.9	0.2165	2.4	0.9	2.6	0.0973	5.2	1.1	5.3
7.5 – 10	1.0227	1.9	1.6	2.5	0.2524	1.9	0.9	2.1	0.1292	3.5	1.1	3.7
10 –12.5	1.0107	1.4	1.6	2.1	0.2516	1.4	0.9	1.7	0.1361	2.4	1.1	2.6
12.5 – 15	1.0964	1.2	1.6	2.0	0.2544	1.3	0.9	1.6	0.1374	2.1	1.1	2.4
15 – 20	1.2889	0.7	1.6	1.7	0.2401	0.8	0.9	1.2	0.1620	1.2	1.1	1.6
20 – 25	1.3724	0.6	1.6	1.7	0.2577	0.7	0.9	1.1	0.1510	1.1	1.1	1.6
25 – 30	1.3310	0.5	1.6	1.7	0.2399	0.6	0.9	1.1	0.1443	0.9	1.1	1.4
30 – 40	1.2761	0.4	1.6	1.6	0.2389	0.5	0.9	1.0	0.1285	0.7	1.1	1.3
40 – 50	1.3144	0.4	1.6	1.6	0.2239	0.5	0.9	1.0	0.1282	0.8	1.1	1.4
50 – 60	1.2572	0.4	1.6	1.6	0.2056	0.5	0.9	1.0	0.1306	0.7	1.1	1.3
60 – 80	1.2093	0.3	1.6	1.6	0.2151	0.4	0.9	1.0	0.1226	0.7	1.1	1.3
80 – 100	1.1882	0.3	1.6	1.6	0.2104	0.5	0.9	1.0	0.1317	0.7	1.1	1.3
100 – 120	1.1473	0.4	1.6	1.6	0.2151	0.5	0.9	1.0	0.1228	0.7	1.1	1.3
120 – 150	1.0911	0.6	1.6	1.7	0.2142	0.7	0.9	1.1	0.1286	1.1	1.1	1.6
150 – 175	1.0527	0.6	1.6	1.7	0.2170	0.8	0.9	1.2	0.1315	1.1	1.1	1.6
175 – 200	1.0298	0.7	1.6	1.7	0.2129	0.8	0.9	1.2	0.1361	1.2	1.1	1.6
200 – 225	1.0241	1.0	1.6	1.9	0.2228	1.1	0.9	1.4	0.1398	1.4	1.1	1.8

[a] Energy bins as used for calculating the Maxwellian averaged cross sections

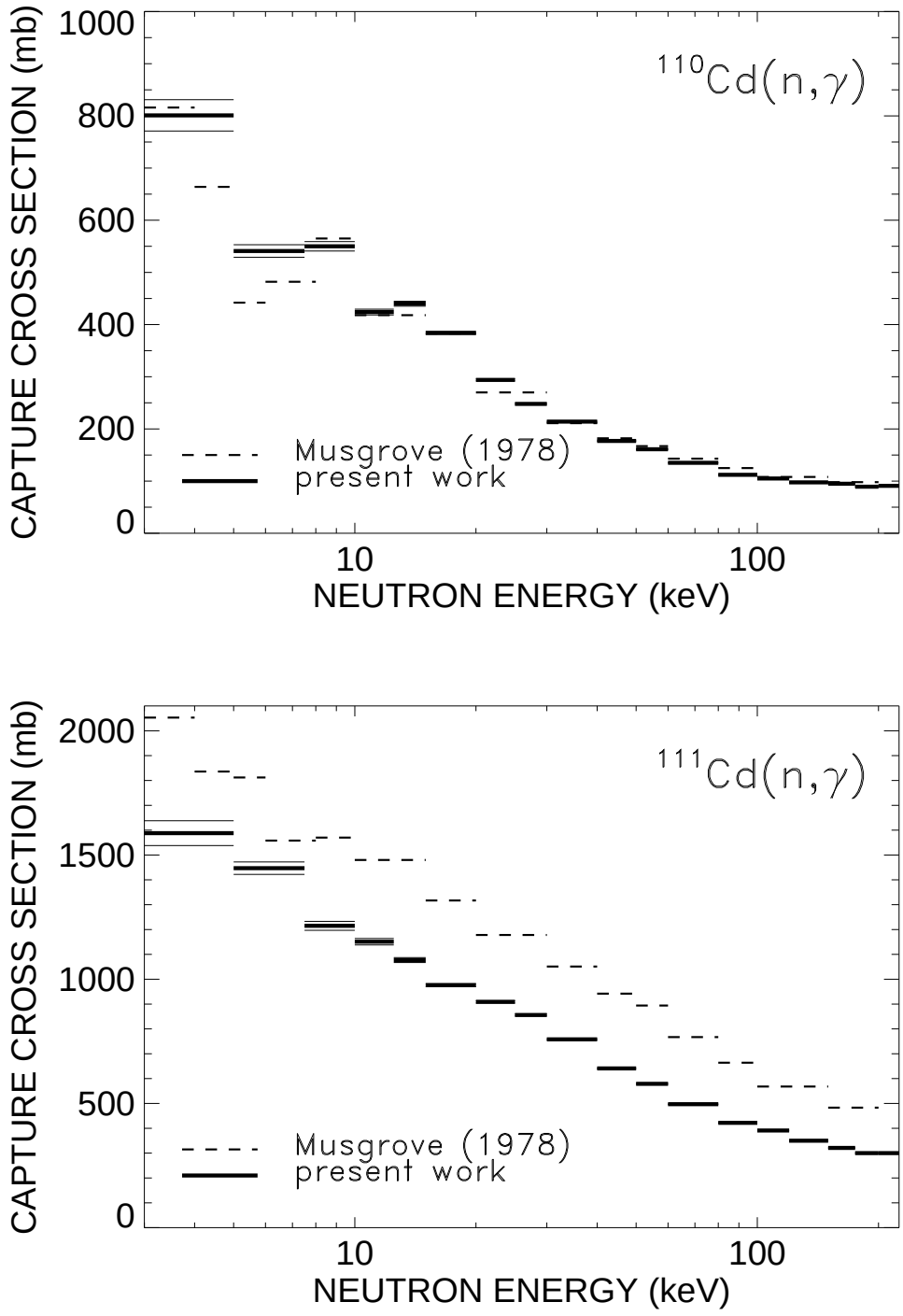

Figure 10: The neutron capture cross sections of ^{110}Cd and ^{111}Cd compared to the data of Musgrove *et al.* [2, 3, 4].

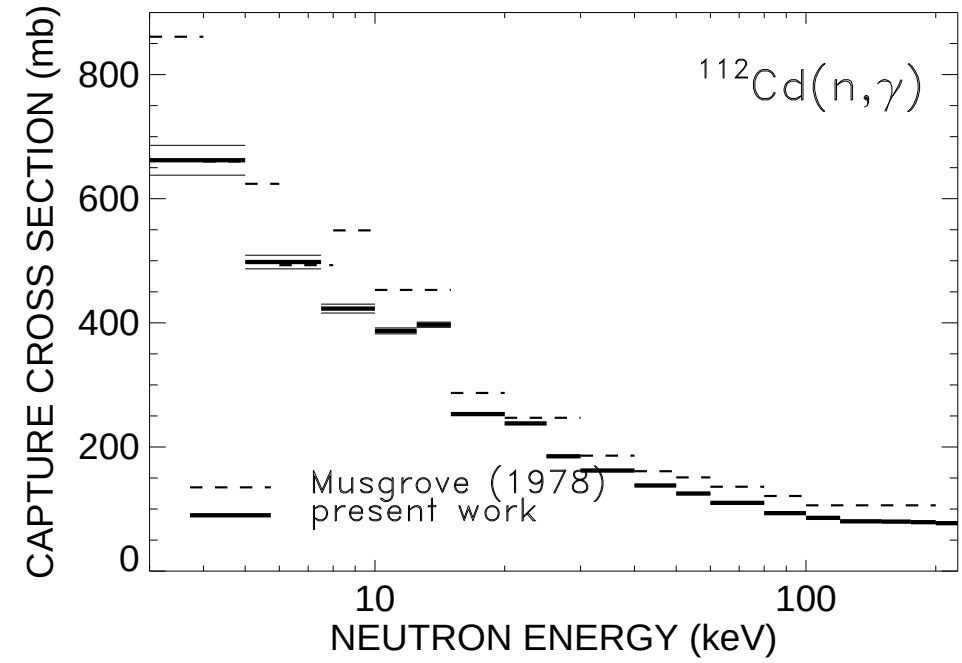

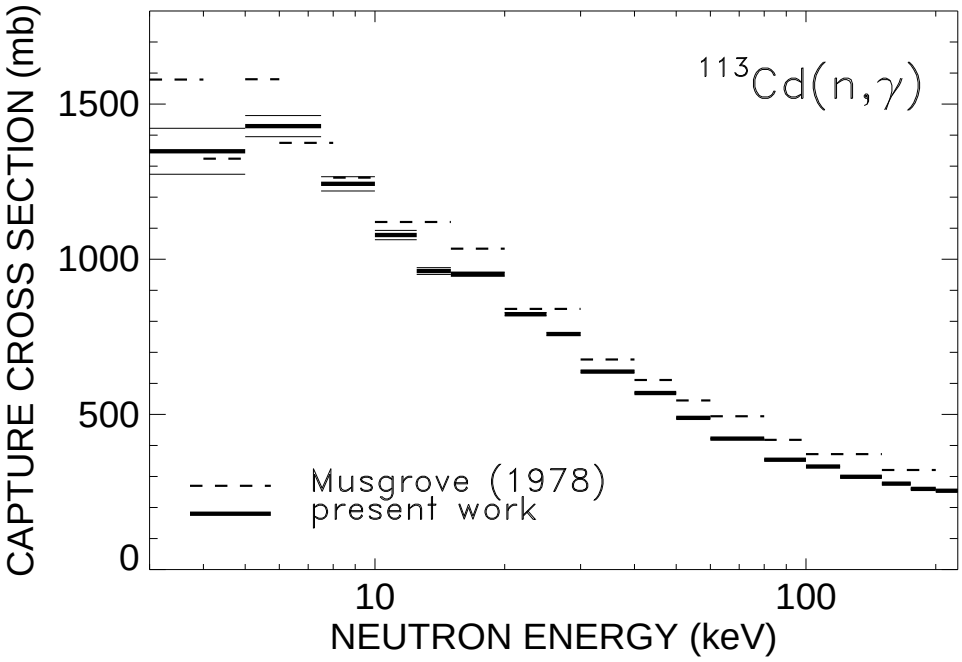

Figure 11: Same as Fig. 10 but for ^{112}Cd and ^{113}Cd.

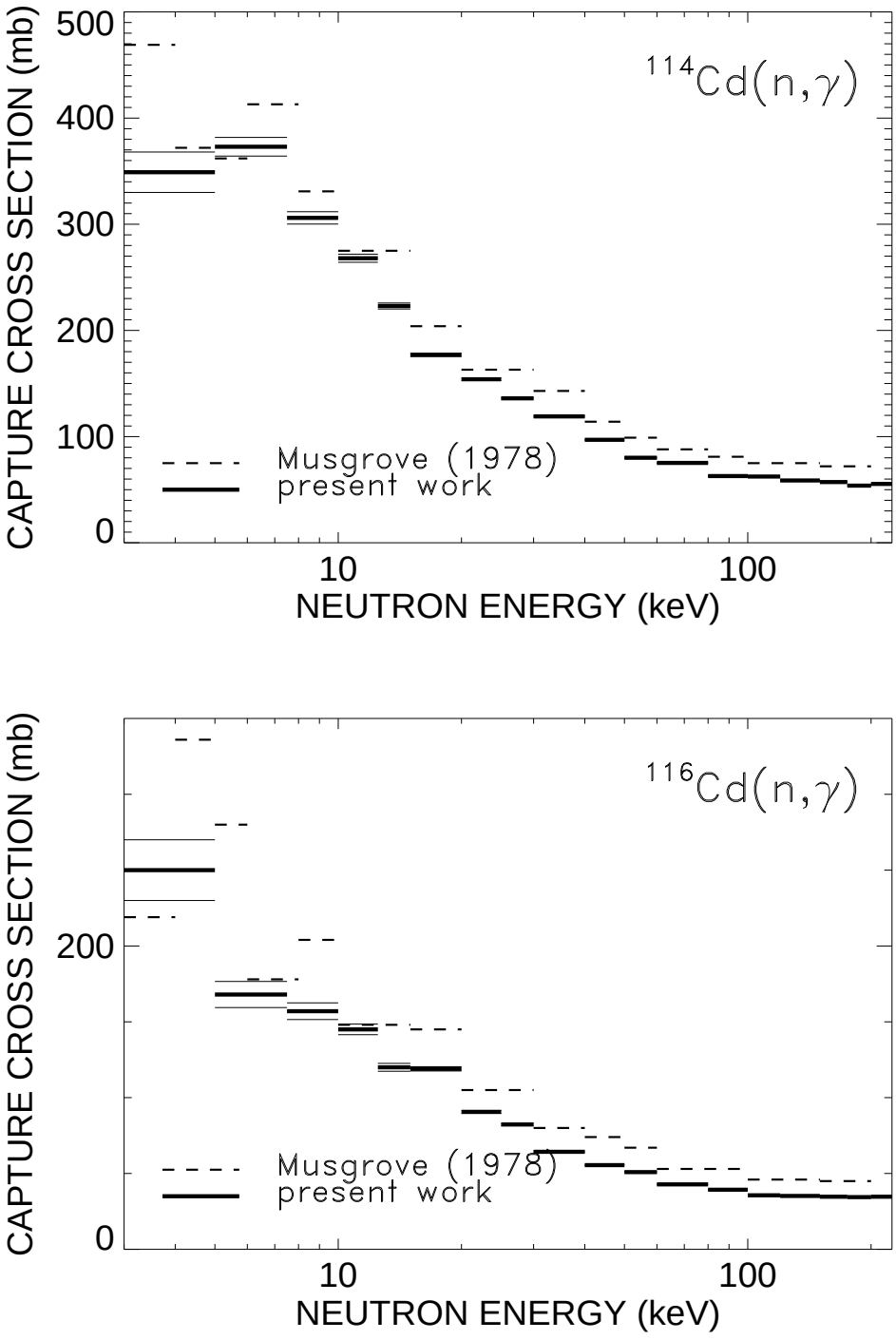

Figure 12: Same as Fig. 10 but for ^{114}Cd and ^{116}Cd.

Table 19: NEUTRON CAPTURE CROSS SECTIONS OF ^{110}Cd, ^{111}Cd,^{112}Cd, ^{113}Cd, ^{114}Cd, AND ^{116}Cd (in mb).

Energy Bin[a] (keV)	$\sigma(^{197}\mathrm{Au})^b$	$\sigma(^{110}\mathrm{Cd})$	$\sigma(^{111}\mathrm{Cd})$	$\sigma(^{112}\mathrm{Cd})$	$\sigma(^{113}\mathrm{Cd})$	$\sigma(^{114}\mathrm{Cd})$	$\sigma(^{116}\mathrm{Cd})$
3 – 5	2266.7	801.5	1589.	662.0	1348.	349.5	250.0
5 – 7.5	1726.7	541.7	1447.	498.2	1430.	373.8	168.1
7.5 – 10	1215.7	550.7	1216.	423.6	1243.	306.8	157.1
10 – 12.5	1066.7	424.0	1151.	387.8	1078.	268.4	145.2
12.5 – 15	878.0	440.2	1078.	397.6	962.7	223.3	120.7
15 – 20	738.8	384.4	976.8	253.8	952.2	177.4	119.7
20 – 25	600.0	294.6	909.8	238.9	823.5	154.7	90.6
25 – 30	570.8	248.9	856.2	185.4	759.8	137.0	82.3
30 – 40	500.4	214.4	758.4	162.5	638.5	119.6	64.3
40 – 50	433.3	177.6	641.6	138.2	569.6	97.0	55.5
50 – 60	389.6	161.0	579.6	125.9	489.9	80.1	50.9
60 – 80	349.4	134.8	497.1	110.0	422.5	75.2	42.8
80 – 100	298.3	112.1	422.5	93.4	354.5	62.8	39.3
100 – 120	290.1	105.3	391.2	85.8	332.9	62.4	35.6
120 – 150	274.1	97.6	350.7	80.2	299.1	58.7	35.3
150 – 175	263.7	94.9	321.9	79.7	277.5	57.2	34.7
175 – 200	252.6	89.3	300.7	78.8	260.1	53.8	34.4
200 – 225	248.5	90.9	299.9	77.3	254.5	55.4	34.7

[a] As used for calculating the Maxwellian averaged cross sections
[b] Based on the ^{197}Au data from literature[20, 21]

5 DISCUSSION OF UNCERTAINTIES

Since the determination of statistical and systematic uncertainties in measurements with the 4π BaF_2 detector has been described in Refs. [8, 9, 11], the following discussion concentrates on the particular aspects of the present experiment. The various uncertainties are compiled in Table 20.

The binding energy for the even isotopes is sufficiently low for normalizing the scattering background in the sum energy region around 9 MeV. Therefore, no systematic differences were observed in the data, neither between individual runs nor correlated with the different acquisition modes or evaluation methods (see Tables 12 to 17). Accordingly, systematic uncertainties in background subtraction were negligible as in the measurements on the samarium [8], gadolinium [22], and dysprosium [16] isotopes. For the odd isotopes, however, the high binding energy made it necessary to use the peak due to capture on the even barium isotopes at 6.8 MeV for normalization. This comparably weak peak being

situated on the tail of the spectrum from true events, implies non-negligible systematic uncertainties for this correction. This difficulty may explain the 1% variation in the ^{113}Cd results obtained in different runs. Therefore, a conservative systematic uncertainty of 1% was assumed for this effect for both odd isotopes.

The systematic uncertainties related to the flight path measurement and the neutron flux normalization have been discussed previously.

The samples were slightly contaminated by several other metals at the level of about 50 ppm, but the total contamination was less than 0.04% in all cases. Since most of these elements were known to have smaller capture cross sections than Cd, a systematic uncertainty of 0.1% was sufficient to account for these impurities.

The isotopic composition (Table 2) was specified with an absolute uncertainty of <0.2% for the main isotope and of <0.1% for the impurity isotopes in each sample. Though these seem to be rather conservative numbers [23] they were adopted in data analysis, resulting in a relative uncertainty of 0.2% for the mass of the main isotopes in the highly enriched samples. The uncertainty related to the isotopic correction has been discussed in detail elsewhere [16, 22]. Accordingly, the small isotopic corrections of the present experiment give rise to uncertainties of 0.2% for all isotopes.

Because of the high enrichment to more than 95%, the correction for neutron multiple scattering and self-shielding could be calculated by the assumption that the effect due to impurity isotopes was accounted for by the isotopic correction, i.e. assuming that the sample contained only the main isotope. The uncertainties quoted in Table 20 are those provided by the SESH code [12] (see also Table 11).

The detailed discussion of the systematic uncertainties due to undetected events for the gadolinium experiment [22] showed that uncertainties of the correction factor F_1 were 0.3% for the even and 0.8% for the odd isotopes. These corrections were based on two independent sets of calculated capture cascades, and were found to agree with the respective uncertainties quoted in previous measurements with the 4π BaF_2 detector [8, 9, 19]. It turned out that this uncertainty was mainly determined by the difference in binding energy between the investigated isotope and the gold standard, which is large for the odd, but small for the even gadolinium isotopes. This result was verified by using experimental capture cascades from capture on various dysprosium isotopes [16], thus confirming the reliability of the evaluated uncertainties. Compared to the gadolinium case the binding energies of the cadmium isotopes relative to gold are slightly larger for the even, but much larger for the odd isotopes. Therefore, systematic uncertainties of 0.4% and 1.1% were adopted for the even and odd isotopes, respectively.

6 MAXWELLIAN AVERAGED CROSS SECTIONS

Maxwellian averaged cross sections were calculated in the same way as described in Refs. [9, 11]. The neutron energy range from 0 - 700 keV was divided into three intervals I_x according to the origin of the adopted cross sections (see Table 21). The dominant part I_2 between 3 and 225 keV is provided by the present experiment (Table 19). These data were

Table 20: SYSTEMATIC UNCERTAINTIES (%)

Background subtraction (^{111,113}Cd)	1.0
Flight path	0.1
Neutron flux normalization	0.2
Sample mass: elemental impurities	0.1
Isotopic composition	0.2
Isotopic correction	0.2
Multiple scattering and self–shielding: F_2	
cross section ratio (^{110}Cd/^{111,113}Cd/^{112}Cd/^{114}Cd/^{116}Cd)	0.5/0.4/0.6/0.7/0.9
Undetected events: F_1	
cross section ratio (even/odd isotopes)	0.4/1.1
total systematic uncertainties	
$\sigma(^{110}\mathrm{Cd})/\sigma(\mathrm{Au})$	0.7
$\sigma(^{111}\mathrm{Cd})/\sigma(\mathrm{Au})$	1.6
$\sigma(^{112}\mathrm{Cd})/\sigma(\mathrm{Au})$	0.8
$\sigma(^{113}\mathrm{Cd})/\sigma(\mathrm{Au})$	1.6
$\sigma(^{114}\mathrm{Cd})/\sigma(\mathrm{Au})$	0.9
$\sigma(^{116}\mathrm{Cd})/\sigma(\mathrm{Au})$	1.1

obtained with sufficient resolution in neutron energy to exclude systematic uncertainties that may result in the calculation of the Maxwellian average if the energy grid is too coarse.

The contribution I_1 was determined by normalizing the cross sections of Kopecky *et al.* [24] to the present data in the interval between 3 to 15 keV. The shape of both data sets were found in good agreement, yielding consistent normalization constants in the five energy bins considered. Accordingly, an uncertainty of 5% was obtained for the contribution I_1.

At typical *s*-process temperatures the energy interval from 225 to 700 keV contributes very little to the Maxwellian average. For this part, the data of Kopecky *et al.* [24] were normalized to the present results between 50 and 225 keV, and the corresponding uncertainties were assumed to increase from 2% at 225 keV to 10% at 700 keV.

The systematic uncertainties of the Maxwellian averaged cross sections in Table 21 are determined by the uncertainties of the measured cross section ratios in the interval I_2 (Table 18) as well as by the respective I_1 and I_3 contributions. The 1.5% uncertainty of the gold standard was not included since it cancels out in most applications of relevance for *s*-process studies. In general, the systematic uncertainties dominate over the statistical uncertainties, except for the even isotopes at low thermal energies.

The present results at kT=30 keV are eventually compared in Table 22 with previous experiments and with the compilations of Bao *et al.* [1] and Beer, Voss, and Winters [25]. The comparison with the data of Musgrove *et al.* has already been discussed for

the energy dependent cross sections. For ^{114}Cd there is excellent agreement with a recent activation measurement by Theis *et al.* [6]. Using natural Cd samples, Theis *et al.* were able to deduce the ^{116}Cd cross section in the same experiment. In this case, however, they report a 27% smaller value than obtained in the present measurement, a discrepancy which seems to originate from a problem with their adopted γ-intensities for the decay of the product nucleus ^{117}Cd.

7 ACKNOWLEDGEMENTS

We are indebted to E.P. Knaetsch, D. Roller and W. Seith for operating the Van de Graaff accelerator as to provide excellent beam conditions throughout the entire experiment. We also thank G. Rupp for his invaluable technical assistance which was essential for the success of this work as well as D. Petrich for his help with the figures. The hospitality of Forschungszentrum Karlsruhe is gratefully acknowledged by L.K.

Table 21: MAXWELLIAN AVERAGED NEUTRON CAPTURE CROSS SECTIONS OF THE CADMIUM ISOTOPES.

^{110}Cd							
ΔE	0 - 3 keV	3 - 225 keV	225 - 700 keV	Thermal Spectrum			
Data:	from Ref. [24][a]	this work	from Ref. [24][a]				
kT	I_1	I_2	I_3	$<\sigma v>/v_T$ (mbarn)			
(keV)	(mbarn)	(mbarn)	(mbarn)		stat	sys[b]	tot
8	60.6±3.0	452.3±3.6	0.0	512.9	4.7	3.6	5.9
10	40.4±2.0	415.1±2.7	0.0	455.5	3.4	3.2	4.7
15	18.9±0.9	342.2±1.7	0.0	361.1	1.9	2.5	3.1
20	10.9±0.5	292.5±1.2	0.0	303.4	1.3	2.1	2.5
25	7.1±0.4	257.2±1.0	0.1	264.4	1.1	1.9	2.2
30	5.0±0.3	231.0±0.8	0.5	236.5	0.9	1.7	1.9
40	2.8±0.1	194.0±0.6	2.3±0.1	199.1	0.6	1.4	1.5
50	1.8±0.1	167.9±0.5	5.9±0.2	175.6	0.5	1.2	1.3
52	1.7±0.1	163.5±0.5	6.8±0.2	172.0	0.5	1.2	1.3
60	1.3±0.1	147.6±0.4	10.8±0.3	159.7	0.5	1.1	1.2
70	0.9±0.0	131.0±0.4	16.4±0.6	148.3	0.7	1.0	1.2
80	0.7±0.0	116.9±0.4	22.1±0.8	139.7	0.9	1.0	1.3
90	0.6±0.0	104.9±0.3	27.7±1.1	133.2	1.1	0.9	1.4
100	0.5±0.0	94.5±0.3	32.8±1.3	127.8	1.3	0.9	1.6
^{111}Cd							
ΔE	0 - 3 keV	3 - 225 keV	225 - 700 keV	Thermal Spectrum			
Data:	from Ref. [24][a]	this work	from Ref. [24][a]				
kT	I_1	I_2	I_3	$<\sigma v>/v_T$ (mbarn)			
(keV)	(mbarn)	(mbarn)	(mbarn)		stat	sys[b]	tot
8	173.2±8.7	1162.±6.7	0.0	1335.	11.	21.	24.
10	115.6±5.8	1106.±5.3	0.0	1222.	7.9	20.	22.
15	54.3±2.7	979.6±3.5	0.0	1034.	4.4	17.	18.
20	31.4±1.6	880.0±2.6	0.0	911.4	3.1	15.	15.
25	20.5±1.0	801.8±2.2	0.4	822.7	2.4	13.	13.
30	14.4±0.7	738.7±1.9	1.3	754.4	2.0	12.	12.
40	8.2±0.4	640.8±1.5	6.5±0.2	655.5	1.6	10.	10.
50	5.3±0.3	564.9±1.3	15.8±0.4	586.0	1.4	9.4	9.5
52	4.9±0.2	551.4±1.3	18.1±0.5	574.4	1.4	9.2	9.3
60	3.7±0.2	501.9±1.2	27.8±0.8	533.4	1.5	8.5	8.6
70	2.7±0.1	448.1±1.1	40.5±1.3	491.3	1.7	7.9	8.1
80	2.1±0.1	401.6±1.0	52.6±1.7	456.3	2.0	7.3	7.6
90	1.7±0.1	361.3±0.9	63.4±2.2	426.4	2.4	6.8	7.2
100	1.3±0.1	326.2±0.8	72.7±2.6	400.2	2.7	6.4	6.9

Table 21 (continued)

^{112}Cd							
ΔE	0 - 3 keV	3 - 225 keV	225 - 700 keV	Thermal Spectrum			
Data:	from Ref. [24][a]	this work	from Ref. [24][a]				
kT	I_1	I_2	I_3	$<\sigma v>/v_T$ (mbarn)			
(keV)	(mbarn)	(mbarn)	(mbarn)		stat	sys[b]	tot
8	49.8±2.5	369.7±3.0	0.0	419.5	3.9	3.4	5.2
10	33.3±1.7	335.7±2.3	0.0	369.0	2.9	3.0	4.2
15	15.7±0.8	272.7±1.4	0.0	288.4	1.6	2.3	2.8
20	9.1±0.5	231.9±1.0	0.0	241.0	1.1	1.9	2.2
25	5.9±0.3	203.8±0.8	0.1	209.8	0.9	1.7	1.9
30	4.2±0.2	183.3±0.7	0.4	187.9	0.7	1.5	1.7
40	2.4±0.1	154.7±0.5	2.0±0.1	159.1	0.5	1.3	1.4
50	1.5±0.1	134.6±0.4	5.1±0.1	141.2	0.4	1.1	1.2
52	1.4±0.1	131.2±0.4	5.9±0.2	138.5	0.5	1.1	1.2
60	1.1±0.1	118.9±0.4	9.4±0.3	129.4	0.5	1.0	1.1
70	0.8±0.0	105.9±0.3	14.2±0.5	120.9	0.6	1.0	1.2
80	0.6±0.0	94.9±0.3	19.2±0.7	114.7	0.8	0.9	1.2
90	0.5±0.0	85.3±0.3	23.9±0.9	109.7	0.9	0.9	1.3
100	0.4±0.0	77.1±0.3	28.3±1.1	105.8	1.1	0.8	1.4
^{113}Cd							
ΔE	0 - 3 keV	3 - 225 keV	225 - 700 keV	Thermal Spectrum			
Data:	from Ref. [24][a]	this work	from Ref. [24][a]				
kT	I_1	I_2	I_3	$<\sigma v>/v_T$ (mbarn)			
(keV)	(mbarn)	(mbarn)	(mbarn)		stat	sys[b]	tot
8	149.0±7.5	1087.±9.0	0.0	1236.	12.	20.	23.
10	99.5±5.0	1027.±6.9	0.0	1127.	8.5	18.	20.
15	46.9±2.3	893.5±4.2	0.0	940.4	4.8	15.	16.
20	27.2±1.4	792.1±3.0	0.0	819.3	3.3	13.	13.
25	17.7±0.9	714.6±2.4	0.3	732.6	2.6	12.	12.
30	12.4±0.6	653.6±2.0	1.3	667.3	2.1	11.	11.
40	7.1±0.4	561.6±1.5	6.5±0.2	575.2	1.6	9.2	9.3
50	4.6±0.2	492.1±1.3	16.5±0.5	513.2	1.4	8.2	8.3
52	4.2±0.2	480.0±1.3	19.0±0.6	503.2	1.4	8.1	8.2
60	3.2±0.2	435.6±1.1	30.0±0.9	468.8	1.4	7.5	7.6
70	2.4±0.1	388.0±1.0	45.2±1.5	435.6	1.8	7.0	7.2
80	1.8±0.1	347.2±0.9	60.4±2.1	409.4	2.3	6.6	7.0
90	1.4±0.1	311.9±0.8	74.9±2.8	388.2	2.9	6.2	6.8
100	1.2±0.1	281.3±0.8	88.0±3.5	370.5	3.6	5.9	6.9

Table 21 (continued)

^{114}Cd							
ΔE	0 - 3 keV	3 - 225 keV	225 - 700 keV	Thermal Spectrum			
Data:	from Ref. [24][a]	this work	from Ref. [24][a]				
kT	I_1	I_2	I_3	$<\sigma v>/v_T$ (mbarn)			
(keV)	(mbarn)	(mbarn)	(mbarn)		stat	sys[b]	tot
8	39.3±2.0	246.5±2.4	0.0	285.8	3.1	2.6	4.0
10	26.2±1.3	225.3±1.8	0.0	251.5	2.2	2.3	3.2
15	12.3±0.6	184.8±1.1	0.0	197.1	1.3	1.8	2.2
20	7.1±0.4	158.0±0.8	0.0	165.1	0.9	1.5	1.7
25	4.6±0.2	139.3±0.6	0.1	144.0	0.6	1.3	1.4
30	3.2±0.2	125.7±0.5	0.3	129.2	0.5	1.2	1.3
40	1.9±0.1	106.6±0.4	1.4	109.9	0.4	1.0	1.1
50	1.2±0.1	93.1±0.4	3.6±0.1	97.9	0.4	0.9	1.0
52	1.1±0.1	90.8±0.3	4.1±0.1	96.0	0.3	0.9	0.9
60	0.8±0.0	82.5±0.3	6.5±0.2	89.8	0.4	0.8	0.9
70	0.6±0.0	73.6±0.3	9.9±0.3	84.1	0.4	0.8	0.9
80	0.5±0.0	66.0±0.3	13.4±0.5	79.9	0.6	0.7	0.9
90	0.4±0.0	59.5±0.2	16.7±0.6	76.6	0.6	0.7	0.9
100	0.3±0.0	53.8±0.2	19.7±0.8	73.8	0.8	0.7	1.1
^{116}Cd							
ΔE	0 - 3 keV	3 - 225 keV	225 - 700 keV	Thermal Spectrum			
Data:	from Ref. [24][a]	this work	from Ref. [24][a]				
kT	I_1	I_2	I_3	$<\sigma v>/v_T$ (mbarn)			
(keV)	(mbarn)	(mbarn)	(mbarn)		stat	sys[b]	tot
8	20.2±1.0	138.8±2.4	0.0	159.0	2.6	1.7	3.1
10	13.5±0.7	127.6±1.8	0.0	141.1	1.9	1.6	2.5
15	6.4±0.3	105.7±1.1	0.0	112.1	1.1	1.2	1.6
20	3.7±0.2	90.9±0.8	0.0	94.6	0.8	1.0	1.3
25	2.4±0.1	80.5±0.6	0.0	82.9	0.6	0.9	1.1
30	1.7±0.1	72.9±0.5	0.2	74.8	0.5	0.8	0.9
40	1.0±0.1	62.2±0.4	0.9	64.1	0.4	0.7	0.8
50	0.6±0.0	54.7±0.3	2.4±0.1	57.7	0.3	0.6	0.7
52	0.6±0.0	53.4±0.3	2.7±0.1	56.7	0.3	0.6	0.7
60	0.4±0.0	48.7±0.3	4.3±0.1	53.4	0.3	0.6	0.7
70	0.3±0.0	43.6±0.3	6.5±0.2	50.4	0.4	0.6	0.7
80	0.2±0.0	39.2±0.2	8.8±0.3	48.2	0.4	0.5	0.6
90	0.2±0.0	35.4±0.2	10.9±0.4	46.5	0.4	0.5	0.6
100	0.2±0.0	32.1±0.2	12.9±0.5	45.2	0.5	0.5	0.7

[a]Normalized to present data

[b]The 1.5% uncertainty of the gold standard is not included here, since it cancels out in most applications of relevance for nuclear astrophysics

Table 22: MAXWELLIAN AVERAGED CROSS SECTIONS AT kT=30 keV COMPARED TO PREVIOUS EXPERIMENTS AND EVALUATIONS

Isotope	Experiment		Evaluation	
	Cross section (mb)	Reference	Bao *et al.* [1]	Beer, Voss, Winters [25]
^{110}Cd	236.5 ± 1.9	present work[a]	246±30	246±30
	236 ± 30	Musgrove *et al.* (78)[b] [3]		
	246 ± 30	Musgrove *et al.* (78)[b] [2]		
	270 ± 30	Stroud (72) [5]		
^{111}Cd	754.4 ± 12.0	present work[a]	1063±125	1063±125
	1063 ± 125	Musgrove *et al.* (78)[b] [3]		
^{112}Cd	187.9 ± 1.7	present work[a]	235 ±30	233 ±30
	222 ± 30	Musgrove *et al.* (78)[b] [3]		
	235 ± 30	Musgrove *et al.* (78)[b] [2]		
^{113}Cd	667.3 ± 11.0	present work[a]	728±80	728 ± 80
	728 ± 80	Musgrove *et al.* (78)[b] [3]		
^{114}Cd	129.2 ± 1.3	present work[a]	127 ± 5	161 ± 25
	127 ± 5	Theis *et al.* 98 [6]		
	150 ± 25	Musgrove *et al.* (78)[b] [3]		
	161 ± 25	Musgrove *et al.* (78)[b] [2]		
^{116}Cd	74.8± 0.9	present work[a]	59 ± 2	94 ± 12
	59 ± 2	Theis *et al.* (98) [6]		
	94 ±12	Musgrove *et al.* (78)[b] [2]		

[a] The 1.5% uncertainty of the gold cross section is not included, since it cancels out in most applications of relevance for nuclear astrophysics.
[b] These data have been normalized according to Ref. [4].

References

[1] Z.Y. Bao, H. Beer, F. Käppeler, F. Voss, K. Wisshak, and T. Rauscher, Atomic Data Nucl. Data Tables **76**, 70 (2000).

[2] A.R. de L. Musgrove, B.J. Allen, and R.L. Macklin, J. Phys. G: Nucl. Phys. **4**, 771 (1978).

[3] A.R. de L. Musgrove, B.J. Allen, J.W. Boldeman, and R.L. Macklin, in *Neutron Physics and Nuclear Data for Reactors and other Applied Purposes* OECD Paris 1978, p 449.

[4] B.J. Allen, J.W. Boldeman, and R.L. Macklin, Nucl. Sci. Eng. **82**, 230 (1982).

[5] D.B. Stroud, Astrophys. J. **178**, L93 (1972).

[6] Ch. Theis, F. Käppeler, K. Wisshak, and F. Voss, Astrophys. J. **500**, 1039 (1998).

[7] K. Wisshak, F. Voss, C. Arlandini, F. Käppeler, and L. Kazakov, Phys. Rev. C **61**, 065801 (2000).

[8] K. Wisshak, K. Guber, F. Voss, F. Käppeler, and G. Reffo, Phys. Rev. C **48**, 1401 (1993).

[9] K. Wisshak, F. Voss, F. Käppeler, and G. Reffo, Phys. Rev. C **45**, 2470 (1992).

[10] K. Wisshak, K. Guber, F. Käppeler, J. Krisch, H. Müller, G. Rupp, and F. Voss, Nucl. Instr. Meth. A **292**, 595 (1990).

[11] K. Wisshak, F. Voss, F. Käppeler, and G. Reffo, Phys. Rev. C **42**, 1731 (1990).

[12] F. H. Fröhner, Technical report, Gulf General Atomic (unpublished).

[13] C. Nordborg, H. Gruppelaar, and M. Salvatores, in *Nuclear Data for Science and Technology*, edited by S. Qaim (Springer, Berlin, 1992), p. 782.

[14] V. McLane, C.L. Dunford, and P.F. Rose, in *Neutron Cross Sections, Vol. 2,* (Academic Press, New York, 1988).

[15] K. Wisshak, F. Voss, F. Käppeler, L. Kazakov, and G. Reffo, Report FZKA 5967, Forschungszentrum Karlsruhe, Karlsruhe, Germany 1997.

[16] F. Voss, K. Wisshak, C. Arlandini,K. Käppeler, L. Kazakov, and T. Rauscher, Phys. Rev. C **59**, 1154 (1999).

[17] A. Gilbert and A.G.W. Cameron, Can. J. Phys. **43**, 1446 (1965).

[18] J. F. Mughabghab, M. Divadeenam, and N. E. Holden, in *Neutron Cross Sections, Vol. 1, Part A* (Academic Press, New York, 1981).

[19] F. Voss, K. Wisshak, K. Guber, F.Käppeler, and G. Reffo, Phys. Rev. C **50**, 2582 (1994).

[20] R. L. Macklin, private communication (unpublished).

[21] W. Ratynski and F. Käppeler, Phys. Rev. C **37**, 595 (1988).

[22] K. Wisshak, F. Voss, F. Käppeler, K. Guber, L. Kazakov, N. Kornilov, M. Uhl, and G. Reffo, Phys. Rev. C. **52**, 2762 (1995).

[23] K. Wisshak, F. Voss, F. Käppeler, L. Kazakov, and G. Reffo, Phys. Rev. C. **57**, 391 (1998).

[24] J. Kopecky, J.-Ch. Sublet, J.A. Simpson, R.A. Forrest, and D. Nierop, Report INDC(NDS)-362, International Atomic Energy Agency, Vienna, Austria, 1997.

[25] H. Beer, F. Voss, and R.R. Winters, Astrophys. J. Suppl. **80**, 403 (1992).